Research Square

Preprints are preliminary reports that have not undergone peer review.
They should not be considered conclusive, used to inform clinical practice,
or referenced by the media as validated information.

# Partial composite action in prestressed UHPC-NC composite girders: interface characterisation, prestress gain and a conservative assessment of a bond-based check

**Yuzhe Tang**

609052897@qq.com

Hunan Technical College of Railway High-speed

**Research Article**

**Keywords:** partial composite action, interfacial bond, UHPC-NC composite girder, prestress gain, bond-slip stiffness

**Posted Date:** November 4th, 2026

**DOI:** https://doi.org/10.21203/rs.3.rs-11437189/v1

**License:** This work is licensed under a Creative Commons Attribution 4.0 International License.
Read Full License

**Additional Declarations:** No competing interests reported.

# Partial composite action in prestressed UHPC-NC composite girders: interface characterisation, prestress gain and a conservative assessment of a bond-based check

**Yuzhe Tang** [1,*]

[1] Hunan Technical College of Railway High-Speed; 609052897@qq.com
* Correspondence: 609052897@qq.com; Tel.: 18890105581

**Abstract**

Prestressed composite girders that pair a UHPC tension layer with normal concrete (NC) are designed as fully bonded, so neither interface slip nor tendon slip enters the calculation. We tested 26 specimens to find out what that costs: eight prestressed girders with the UHPC layer between 160 and 250 mm deep, eight L-shaped direct-shear specimens, and ten damaged beams strengthened with a UHPC layer. Twenty-four of the 26 contain an interface. A load cell at the anchorage measured the tendon force throughout loading and gave a prestress gain of 12.74% of the seated force, reached after the strand had yielded. The direct-shear series separates bare and dowelled joints completely: bare joints fail at 0.98–1.11 times their cracking load, dowelled joints at 5.61–6.01 times, a ratio of 5.53 between the means. No member failed by interface slip. Applying a bond-based partial composite action check to these measurements gives a connection degree of unity in all 16 parameter cases and 0.46–0.57 of the measured capacity. The check reduces to one product, which is the interface quantity a design check would need; a bond strength alone will not serve.

**Keywords:** partial composite action; interfacial bond; UHPC-NC composite girder; prestress gain; bond-slip stiffness

## 1. Introduction

### *1.1 Background*

Bridge girders carry their own weight before they carry anything else, and on a long span that weight sets the depth, the depth adds more weight, and the section can end up sized by a load that does no useful work. Making the section shallower is the obvious answer, but with ordinary concrete the saving is paid for in cracking and durability [2]. Ultra-high performance concrete (UHPC) changes the terms of that trade. A low water-to-binder ratio, a dense matrix and dispersed steel fibres give it tensile capacity and crack control that ordinary concrete does not have, so material can be taken out of the parts of a section that are doing little without losing capacity where it counts [1-3].

Most applications built so far put UHPC in the tension zone and normal concrete (NC) in the compression zone. A monolithic UHPC section would bend just as well, but it would waste material around the neutral axis, where the stress is low and the UHPC contributes almost nothing. The same argument applies in the hogging region of a steel–concrete composite beam, where a UHPC layer in the slab raises the cracking load consid-

erably and changes the ultimate capacity very little, provided the UHPC tension contribution is included in the section resistance [21]. Field applications have accumulated in China. A 50 m simply supported span on the Chahuashan interchange of the Hezhou–Bama expressway in Guangxi uses two longitudinal UHPC webs, each glued from three toothed segments, connected by twelve precast prestressed cross beams and topped by a 75 mm precast soffit form and 165 mm of cast-in-place NC [4]. Designing such a girder is not a matter of adding the two materials together: their shrinkage and creep differ enough that both have to be represented in a serviceability check [5].

*1.2 The partial interaction problem*

All of this assumes that the two layers stay together. AFGC recommendations [6], the fib Model Code [7] and Chinese practice [8] treat the UHPC–NC interface as fully connected, and full connection is convenient: strain stays linear over the depth, the UHPC tensile contribution goes straight into the sectional analysis, and nothing has to be checked at the joint. The difficulty is that a member test cannot show whether the assumption holds. A girder that fails in flexure demonstrates that its section was strong enough; it says nothing about whether the two layers moved together up to that point.

Partial interaction is well established for steel–concrete members and much less so for concrete–concrete joints. Eurocode 4 limits the degree of shear connection to not less than 0.4, because the linear slip assumption behind the model breaks down near full connection; Newmark's formulation, on which that limit rests, assumes a linear-elastic connection and was derived for steel beams, and its extension to concrete–concrete interfaces is recent and still debated [27]. Applying the same treatment to UHPC–NC also requires an interface law, and no accepted expression for the interfacial strength of this material pair exists. A compilation of 563 splitting and 338 slant-shear specimens, with 35 further tests arranged to force debonding, produced a neural-network fit rather than a design formula [28], and two recent reviews report the same gap [29]. Work on precast UHPC girders with cast-in-place decks reaches the same conclusion from the other end: the interface governs, and the code expressions do not reproduce it [30,31].

The first observation concerns the joint itself. Direct shear tests on bonded UHPC–NC interfaces do not give a rigid response: the joint softens after cracking and reaches its peak strength only after slip has begun [9]. Where reinforcement crosses the interface the peak strength rises sharply, but the load at which interface cracking starts falls below that of a roughened or wire-brushed joint, because mechanical interlock has been partly replaced by discrete connectors that engage only once the matrix has cracked [10]. Peak strength and pre-cracking capacity are two different quantities, and the detail that governs one does not govern the other.

The second observation concerns the condition of the member. Beams that need strengthening have usually been in service for decades, and their tensile zone is cracked before the new layer is cast. Almost all published tests, by contrast, use undamaged specimens. Bond between a UHPC overlay and a normal-strength substrate has been characterised over a wide range of surface treatments and exposures [11,12], which settles two of the three variables that matter: surface roughness governs bond strength more than the strength of either material, and exposure governs it in turn, although field trials alongside laboratory tests remain the exception [14]. The third variable is the state of the substrate on the day the new layer is cast, and this is where the characterisation stops. One of the few studies to vary pre-damage as a parameter in its own right tested RC beams strengthened with UHPC layers at different damage levels [13], and its results separate by response. Less pre-damage raises the cracking load and the ultimate load together, because a substrate that has lost less of its tensile resistance keeps more of it under the new layer. A higher reinforcement ratio also raises both, and by more than pre-damage does over the

range tested. Layer thickness works the other way, raising the ultimate load while lowering the cracking load, since a deeper layer spreads the same tensile resultant over more of the section and so delays the cracks the serviceability check is looking for.

### *1.3 Prestress gain and its measurement*

Prestress brings a second uncertainty that is rarely measured. As the girder bends, the strand stretches and its stress rises, so the force at failure is not the force after transfer. Codes handle this with a bond-stress assumption, or by taking the tendon stress at the ultimate limit state as 0.87 of the characteristic strength, which bounds the increment without predicting it. Direct measurements are scarce, and those that exist usually come from strain gauges on the strand or from a model fitted to the test [15], not from a load cell at the anchorage.

This matters because a tendon that gains little stress cannot deliver the crack control the prestress was specified for. If the joint slips, the concrete section strains less, the tendon extends less, and the gain falls. Slip and gain are two readings of the same compatibility condition, which is why both are measured here.

### *1.4 Data-driven approaches and their limits*

Machine learning has been applied widely to the prediction of UHPC member capacity. Gradient-boosted ensembles trained on a database of 218 precast UHPC joints and interpreted with Shapley values have been reported for joint shear capacity, with gradient boosting the best of ten models compared [16]; the same group applied CatBoost, with the same interpretation, to a database of UHPC beams, where the dimensions and the shear span-to-depth ratio dominate and the material and reinforcement parameters follow [17]. A database of a few hundred members supports accurate interpolation inside the domain it covers, and the feature rankings it returns confirm what the design equations already encode: reinforcement area, section depth and material strength dominate, while the post-cracking behaviour of the UHPC enters only weakly, because the published data are too sparse and too varied in fibre configuration to resolve it. A model of this kind returns a number inside a collected domain; it does not say which mechanism produced that number. The mechanism is what interests us here.

### *1.5 Objectives*

The work has four aims.

1. Measure the bonded interface directly, with L-shaped shear tests covering surface preparation, cast-in-place grade and interface reinforcement ratio, and express the result in a form a numerical model can use.

2. Measure the prestress gain of a prestressed UHPC–NC girder during flexural loading, using instrumentation at the anchorage.

3. Compare the two states a real structure can be in: a newly cast girder, where prestress clamps the joint, and a strengthened beam, where it does not.

4. Derive a partial composite action expression, reduce it to the quantities that actually control it, and report how closely it reproduces the measured capacities in both states.

## 2. Conceptual framework

### *2.1. Kinematics of full and partial interaction*

Take a simply supported composite girder of total depth h = + , with a UHPC layer of depth in the tension zone, an NC layer of depth in the compression zone, and a tendon of area , initial stress and modulus . The interface width is .

With full interaction, plane sections remain plane across the joint, the strain is single-valued, the interface carries no slip, and whatever longitudinal force is needed to keep it that way is transferred without question. With partial interaction a slip s opens between the layers, the strains at the joint are no longer equal, and the interface transfers a finite shear flow q over a transfer length. The joint can then fail in one of two ways: it can be too weak to carry the flow the section demands, which is a strength limit, or strong enough but too flexible to develop that flow before opening far enough to use the strength it has, which is a deformation limit. Equations (9) and (11) in Section 7.2 give the connection degree and the mobilised fraction, and the action factor follows from both. Only one of the two limits turns out to be active in the members tested here.

*2.2 The partial composite action factor*

The design consequence of partial interaction is a reduction in the moment obtained from a full-interaction analysis, written as the partial composite action factor ,

$$\eta = \frac{M_{u,true}}{M_{u,full}} \quad (1)$$

which equals unity when both interface checks pass, so that the conventional expression applies unchanged, and falls towards the response of the separated member when either check fails. The separated limit is not the capacity of two layers bending about their own centroids, which is what a linear interpolation would give at = 0. It is a measured quantity, taken here as the ratio of the interface-brittle peak stress to the interlock-dominated peak stress from Series I.

is not a material property. It comes out of a shear flow demand-capacity check, in the same way that the capacity of a stud in a steel-concrete girder does. Section 7.2 shows something less obvious: after substitution the framework depends on the interface through a single product, so one of the two checks drops out in every case examined here.

*2.3 Two states of the same interface*

The argument of this paper is that depends less on how strong the interface is than on what state it is in. Two states are relevant.

In a newly prestressed girder the tendon is tensioned before any external load is applied, and it puts the NC layer in compression. That compression reaches the joint as a permanent normal stress . Any subsequent shear flow is resisted by friction, , and because barely changes with time the joint stays clamped for the whole loading history. The interface is a passive transfer mechanism.

In a girder that has been in service the substrate is already cracked. Cracks crossing the region where the new layer will be cast destroy the interlock the bond depends on and reduce the contact area available for adhesion. The normal compression that prestress would have supplied is absent, because the tendon, if there is one, is not retensioned. The joint then carries whatever the section demands of it across an open crack.

Both states appear in the test programme described below, which is what makes the comparison possible.

## 3. Experimental evidence base

The study draws on three series of tests, described here and reported in full in the companion papers [18-20]. Twenty-six specimens were tested: eight L-shaped interface specimens, eight prestressed composite girders and ten service-damaged strengthened beams. Twenty-four of the 26 contain an interface; the exceptions are the monolithic girders L4-1 and L4-2. The sixteen girders and beams of Series II and III that contain a joint are called interface-bearing members below, with the eight L-shaped specimens counted separately. The series were arranged so that the interface is the common variable: Series I

isolates the interface itself, Series II observes it in a newly prestressed member, and Series III observes it in a service-damaged strengthened member.

### *3.1 Series I: bonded interface specimens*

Series I consists of eight L-shaped specimens tested in direct shear. Each pairs a pre-cast UHPC block with a cast-in-place NC block, measures 500 x 200 x 200 mm overall, and has a nominal shear plane of 250 x 200 mm; the specimens are numbered LI-1 to LI-8. Three of the eight test the surface treatment, a steel wire brush, mechanical roughening by chiselling and vertical dowels, in LI-1, LI-2 and LI-3. Four test the cast-in-place grade, from C30 to C60 at a constant dowel ratio of 0.94 per cent: LI-3 and LI-6 to LI-8. Four test the interface reinforcement ratio, from 0 to 1.57 per cent on a C30 substrate: LI-1 and LI-3 to LI-5. The groups overlap by design, since LI-3 belongs to all three and LI-1 to two of them. Strain gauges on both faces of the shear plane recorded the relative displacement across it, and a servo-hydraulic machine loaded the plane in monotonic compression. Two details of the record matter for Section 4.2: the load steps are of the order of 28 kN, and the displacement channel was transcribed onto a uniform ten-point grid.

Table 1 gives the material properties. The UHPC was tested in flexure and in direct tension, at 17.4 MPa and 11.62 MPa. The cast-in-place concrete was designed to span 30 to 60 MPa, but only one prism was tested, at 33.97 MPa on the C50 substrate, and it is the only prism strength in the programme. Section 5.1 therefore analyses every Series I substrate at the strength derived from that single prism, so the C30, C40 and C60 specimens are not analysed at their own grade; Table 1 lists the cube values for those grades alongside a note that they are not the ones used. The UHPC prism strength of 135.53 MPa is 0.94 of the cube value, the ratio that follows from a 0.85 strength factor on a rectangular stress block. Where a property was not measured, Table 1 says so and the analysis adopts the value stated in Section 5.1.

**Table 1.** Mechanical properties of UHPC and cast-in-place concrete

| Property | Unit | UHPC | NC (C30) | NC (C40) | NC (C50) | NC (C60) |
|---|---|---|---|---|---|---|
| Compressive strength, cube | MPa | 144.2 | 30.0 | 40.0 | 52.6 | 60.0 |
| Compressive strength, prism | MPa | 135.53 | not measured | not measured | 33.97 | not measured |
| Design strength of the substrate, 0.99 | MPa | -- | 29.7 | 39.6 | 33.63 | 59.4 |
| Design strength used in the analysis | MPa | 135.53 | 33.63 | 33.63 | 33.63 | 33.63 |
| Flexural strength, | MPa | 17.4 | not applicable | not applicable | not applicable | not applicable |
| Tensile strength, | MPa | 11.62 | not measured | not measured | not measured | not measured |
| Elastic modulus, | GPa | 46.4 adopted | 35.0 adopted | 35.0 adopted | 34.967 measured | 35.0 adopted |
| Yield strength of reinforcement, $f_y$ | MPa | 442.0 | 442.0 | 442.0 | 442.0 | 442.0 |
| Yield strength of prestressing strand, | MPa | 1820.0 | 1820.0 | 1820.0 | 1820.0 | 1820.0 |
| Ultimate strength of prestressing strand, | MPa | 1975.0 | 1975.0 | 1975.0 | 1975.0 | 1975.0 |

### *3.2 Series II: prestressed UHPC-NC composite girders*

Series II comprises eight prestressed composite girders with a T-section, 2000 mm long and spanning 1800 mm, loaded in four-point bending over a 600 mm constant moment zone. The section is 250 mm deep, with a 200 x 60 mm flange over an 80 mm web, giving a gross area of 27200 mm2. The joint is cast inside the web, so its width is 80 mm rather than the flange width, and that is the width used in every interface calculation below. The NC layer sits in the compression zone above the UHPC layer. A single seven-wire strand of 15.2 mm nominal diameter provides the prestress, tensioned after 28 days of curing; its yield strength is 1820 MPa, its ultimate strength 1975 MPa and its modulus 196 GPa. The UHPC layer depth was 160, 190, 220 or 250 mm, two girders at each depth. The pair at 250 mm is monolithic, with no substrate, and serves as the reference against which the composite girders are judged. Figure 1 shows the elevation, the cross-section and the instrumentation; Table 2 lists the design of both series.

Instrumentation was arranged in four groups. Deflection was measured by displacement transducers at midspan and at the quarter points. Eight strain gauges per face were distributed over the depth at midspan, enough to check whether the strain distribution stayed linear and where it departed from plane sections. A pressure transducer between the strand and the anchor plate at the tensioning end recorded the tendon force continuously through loading, and this is the measurement on which the prestress analysis of Section 6.3 rests. Applied load came from a load cell at the jack, and the prestress was checked by hand calculation. Figure 2 shows the transfer zone and the anchorage.

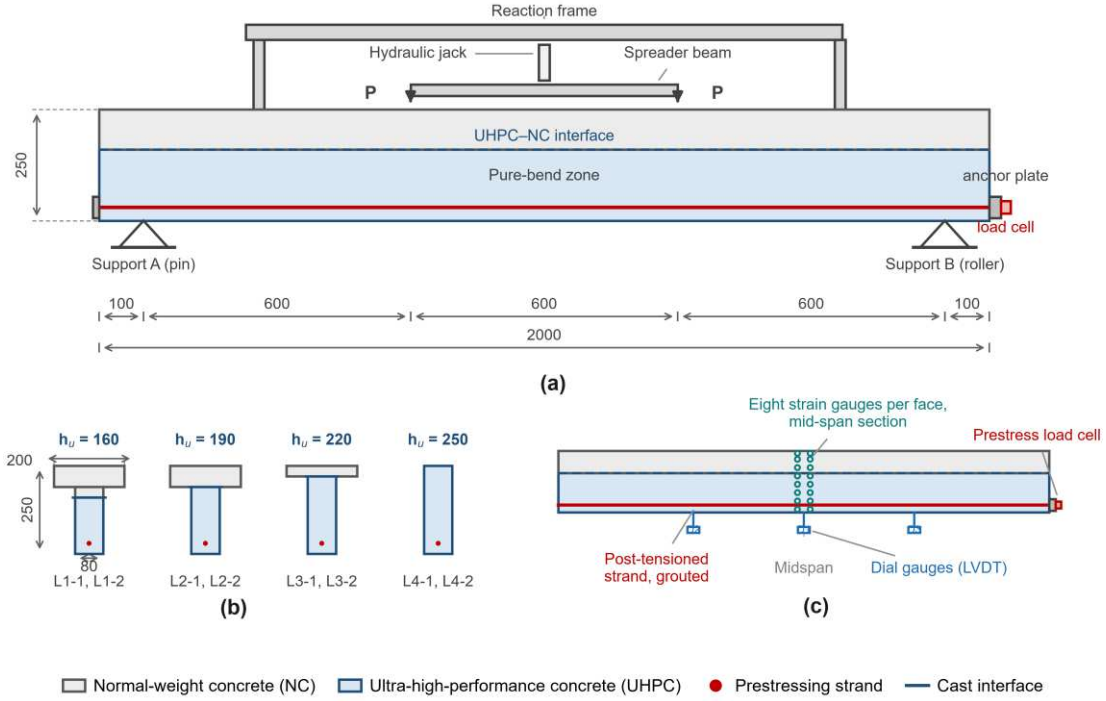



**Figure 1.** Geometry and reinforcement layout of the prestressed composite girders

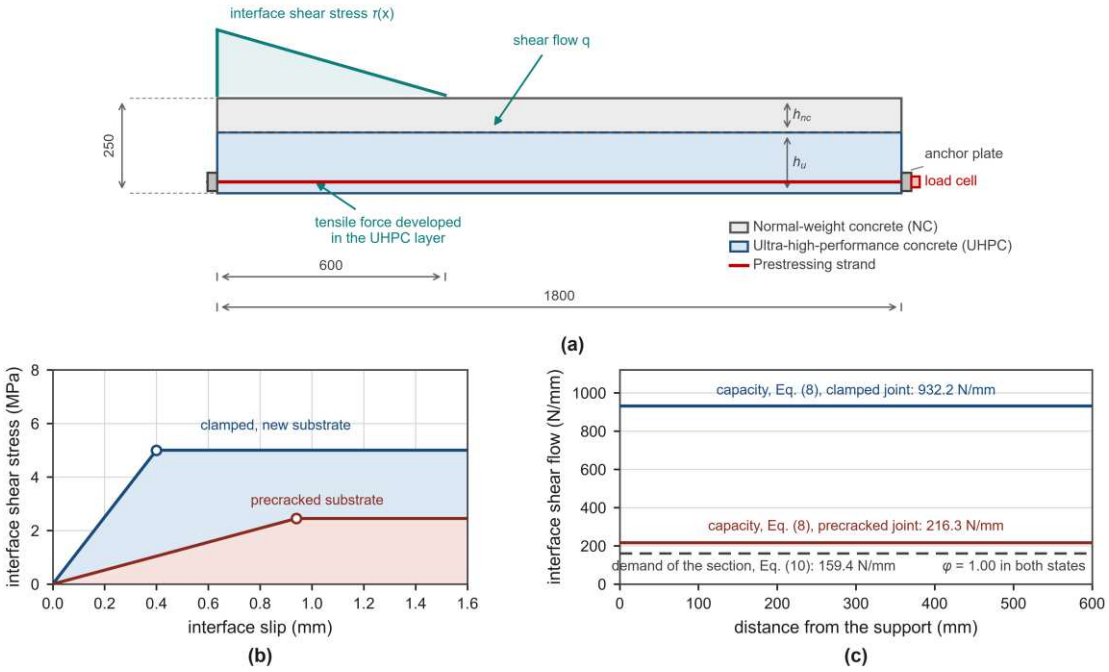



**Figure 2.** Transfer and anchorage of the UHPC-NC composite action.

**Table 2.** Design of the prestressed composite girders (Series II) and the L-shaped interface specimens (Series I).

| Specimen | Form | Key parameters | Target value | Measured response |
|---|---|---|---|---|
| LI-1 to LI-8 | L-shaped, direct shear | Substrate treatment, cast-in-place grade C30 to C60, dowel ratio 0 to 1.57 per cent | Bond-slip characterisation | Peak stress 2.49 to 5.29 MPa; brittle failure in LI-1 and LI-2, ductile in LI-3 to LI-8 |
| L1-1, L1-2 | Prestressed UHPC-NC girder | = 160 mm, = 90 mm, one 15.2 mm seven-wire strand | Partial composite action | 74.88 kN.m, factor 0.915 |
| L2-1, L2-2 | Prestressed UHPC-NC girder | = 190 mm, = 60 mm | Partial composite action | 77.10 kN.m, factor 0.942 |
| L3-1, L3-2 | Prestressed UHPC-NC girder | = 220 mm, = 30 mm | Partial composite action | 79.04 kN.m, factor 0.965 |
| L4-1, L4-2 | Prestressed UHPC-NC girder | = 250 mm, no substrate, monolithic reference | Full composite action, factor 1 by definition | 81.89 kN.m, factor 1.000 |

### *3.3 Series III: service-damaged RC beams strengthened with UHPC*

Ten RC beams, each 2000 mm long, spanning 1800 mm and 250 mm deep, were strengthened with a UHPC layer cast against the soffit and then tested in four-point bending over the same 600 mm constant moment zone. The section is the T of Section 3.2, a 200 x 60 mm flange over an 80 x 190 mm web, so the substrate occupies the lower 200 mm in L1 to L4 and L7 to L10, and the lower 190 mm in L5 and L6, with the joint 80 mm wide throughout. All longitudinal bars were HRB400 of 10 mm diameter. The bars in the new

layer are the variable of Table 3, at 2.05, 2.73 and 3.42 per cent of the layer section; the substrate bars sit 55 mm above the soffit, a nominal 2.73 per cent of the 20000 mm2 web section at the reference beam L3. Corrosion reduces the area and the yield strength of the substrate bars in proportion to the mass lost. Damage was applied in two stages. Precracking came first, by static loading to a level that produced the target crack width in the tension zone, 0, 0.2 or 0.4 mm. Corrosion followed, by immersion in a 5 per cent sodium chloride solution under an impressed current, with the loss of section determined by mass loss. The groups were then arranged so that corrosion rate, layer thickness, reinforcement ratio and precrack width could each be varied on its own.

The reinforcement ratio is quoted against the 20000 mm2 web rather than the 27200 mm2 gross section, because the layer tension is carried in the web and the interface calculation uses the web. The choice affects one result and not the other: the demand on the joint follows from force equilibrium at the limit state and does not depend on the bar area, whereas the computed section capacity does. Section 5.4 gives the resulting bar area, 546 mm2.

**Table 3. Design of the service-damaged UHPC-strengthened beams (Series III).**

| Beam | Corrosion rate (%) | UHPC thickness (mm) | Reinforcement ratio in UHPC layer (%) | Precrack width (mm) |
|---|---|---|---|---|
| L1 | 0 | 50 | 2.73 | 0.2 |
| L2 | 3 | 50 | 2.73 | 0.2 |
| L3 | 8 | 50 | 2.73 | 0.2 |
| L4 | 13 | 50 | 2.73 | 0.2 |
| L5 | 8 | 60 | 2.73 | 0.2 |
| L6 | 8 | 70 | 2.73 | 0.2 |
| L7 | 8 | 50 | 2.05 | 0.2 |
| L8 | 8 | 50 | 3.42 | 0.2 |
| L9 | 8 | 50 | 2.73 | 0.0 |
| L10 | 8 | 50 | 2.73 | 0.4 |

### *3.4 Supplementary data*

Two further data sets are used for context only and are not part of the evidence base. An international review of UHPC in bridge engineering records that field applications now number in the hundreds and that casting a new layer onto an existing member is among the most common forms [22]. A study of shear transfer across such a joint, with a wire brush, a chisel, a groove, dowels, and a groove with dowels, reports the same three failure modes as the L-shaped specimens here: pure interface failure, combined interface and substrate failure, and substrate splitting [24]. A third series on externally prestressed railway T-girders under four axle loads at four operating speeds supplies the service condition in which prestress gain and interface state acquire their practical weight [23].

## 4. Interface characterisation

### *4.1. Failure modes*

The failure mode was set by the surface treatment rather than by the strength of the joint, the first sign that the treatment governs how the member works and not only how

strong it is. The behaviour matches what the bond literature reports for this class of interface. Slant shear tests over five surface textures and three concrete strengths show adequate shear transfer for every texture rougher than 3 mm, whatever the concrete strength [11], and a parallel study across interface angles, curing ages, freeze-thaw exposure and wetting finds the controlling variable to be the early-age strength gain of the UHPC relative to the substrate [12]. Neither study reports a roughness threshold below which the interface fails, which is consistent with the two groups that separate in our series. Wire-brushed and roughened specimens failed in the concrete: cracking started at the surface and ran through the NC matrix while the joint itself stayed largely intact, so the blocks came apart only at large displacement. Dowelled specimens behaved differently. The dowels broke the crack path, and longitudinal cracks parallel to the shear plane split the matrix before any significant slip occurred. The interface shear strength was much higher, but the load at which visible cracking began was lower. Figure 3 shows the two modes.

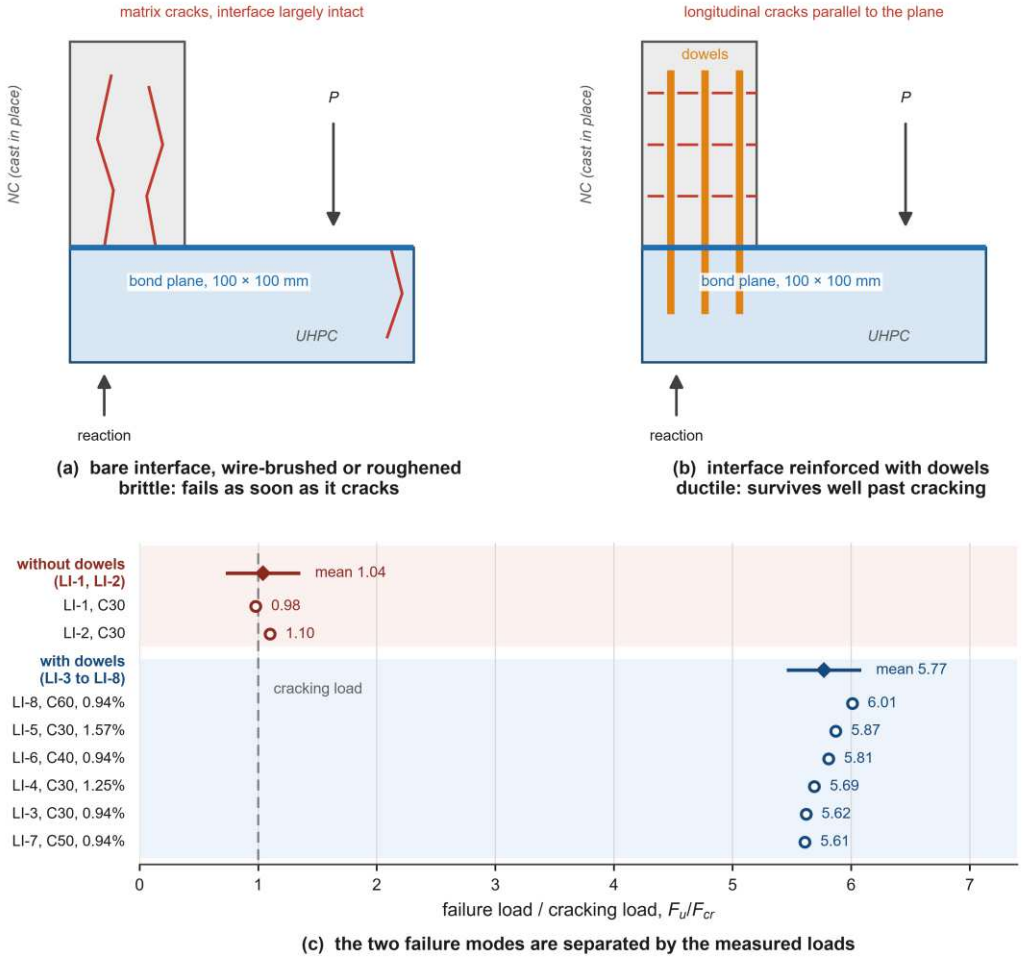



**Figure 3.** Failure of the L-shaped interface specimens

The ratio of failure load to the load at which visible cracking begins separates the two mechanisms completely. The two bare specimens give 0.981 and 1.105, a mean of 1.043: the joint fails at its own cracking load, with no reserve at all. The six dowelled specimens run from 5.606 to 6.011, a mean of 5.767. The ranges do not overlap, the largest bare value being 1.105 against the smallest dowelled value of 5.606, and the ratio of the means is 5.53. This separation belongs to the wider sweep reported in [10], of which our eight specimens are a subset, so the numbers above are a reduction over that subset rather than a new observation. They are also unreplicated, one specimen per condition and two in the bare

group, so no confidence interval can be attached to the ratio. What the subset does show is that the separation survives a different specimen design, since the two families do not overlap within it either.

For the model, the consequence is that a single interface strength will not do. A dowelled joint is strong after cracking and weak before it; a bare joint is the reverse.

### *4.2. Bond-slip response*

The shear stress-slip curves all have the same three stages. In the first the response is linear, cohesion carries the load and no slip is measurable at the loaded face. In the second the matrix at the joint begins to crack, the ascending branch continues at a reduced slope, and slip at the loaded face becomes measurable. In the third the matrix has separated over most of the plane, the response descends, and friction and the dowels, where present, carry what is left. Figure 4 shows the measured curves.

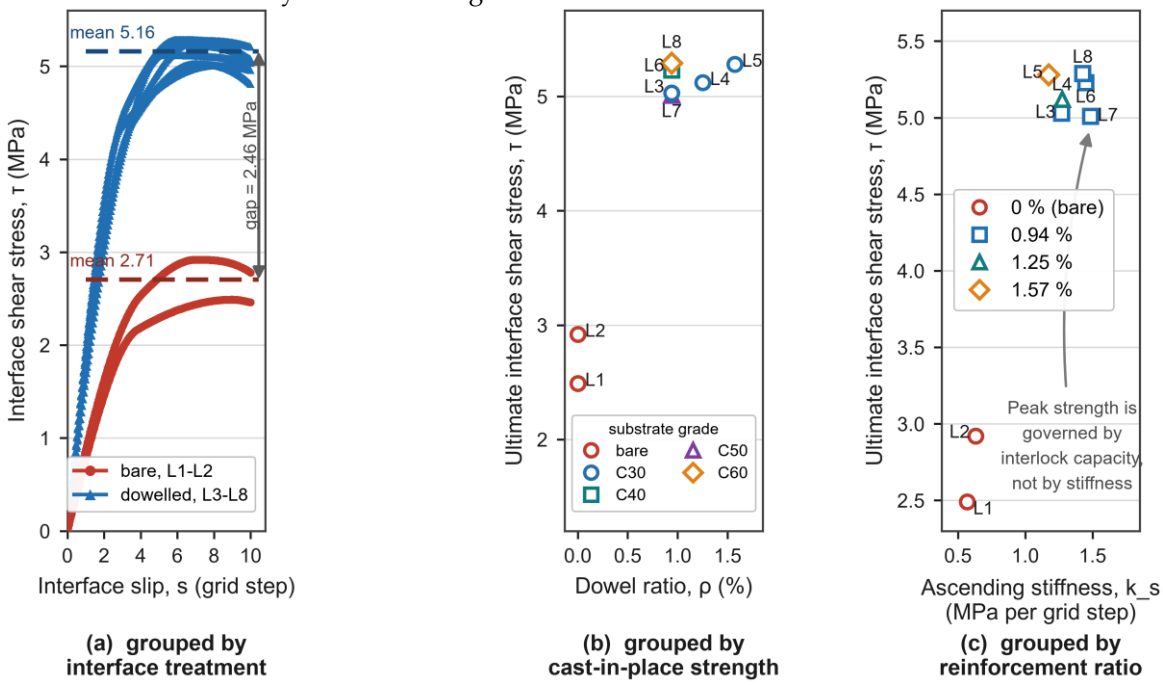



**Figure 4.** Interface shear stress-slip curves for the L-shaped specimens, grouped by interface treatment, cast-in-place strength and interface reinforcement ratio.

Each curve is reduced to four parameters for numerical use: the ascending stiffness , the peak shear stress , the slip at the peak and the residual plateau . Table 4 collects the values derived from these tests.

**Table 4.** Interface parameters derived from the bond-slip curves of Series I

| Group | Treatment | of NC (MPa) | Dowel ratio (%) | on the grid (MPa/step) | adopted (MPa/step) | measured (MPa) | recorded (step) | measured (MPa) | Failure mode |
|---|---|---|---|---|---|---|---|---|---|
| LI-1 | Wire brush | 30 | 0.00 | 0.569 | 0.600 | 2.49 | 9 | 2.46 | brittle |
| LI-2 | Roughened | 30 | 0.00 | 0.632 | 0.600 | 2.92 | 7 | 2.78 | brittle |
| LI-3 | Dowelled, C30, 0.94 % | 30 | 0.94 | 1.270 | 1.346 | 5.03 | 7 | 4.81 | ductile |
| LI-4 | Dowelled, C30, 1.25 % | 30 | 1.25 | 1.274 | 1.346 | 5.12 | 5 | 5.04 | ductile |

| | | | | | | | | | |
|---|---|---|---|---|---|---|---|---|---|
| LI-5 | Dowelled, C30, 1.57 % | 30 | 1.57 | 1.174 | 1.346 | 5.28 | 7 | 5.21 | ductile |
| LI-6 | Dowelled, C40, 0.94 % | 40 | 0.94 | 1.449 | 1.346 | 5.23 | 6 | 5.08 | ductile |
| LI-7 | Dowelled, C50, 0.94 % | 50 | 0.94 | 1.484 | 1.346 | 5.01 | 8 | 4.96 | ductile |
| LI-8 | Dowelled, C60, 0.94 % | 60 | 0.94 | 1.427 | 1.346 | 5.29 | 6 | 5.07 | ductile |

The slip channel was transcribed onto a uniform ten-point grid, and its absolute scale is not recoverable: the load column is irregular, as a recorded signal is, whereas the slip column advances by exactly one unit per row. The two channels therefore share an index that is not a length, and every slip-dependent quantity in Table 4 carries that index. The framework of Section 7 is defined on it and nowhere else.

A stiffness in MPa per mm is a different quantity, and it was not substituted for the grid stiffness. Within the recorded grid the ascending branch is not linear, and its largest secant slope exceeds / by a factor of 1.24 to 2.37 across the eight specimens, so the ratio between a grid stiffness and a stiffness in MPa per mm is not constant and no single length would map one onto the other. A least-squares slope was not used either, because the reinforced specimens change slope once the matrix cracks and a single slope describes neither branch. The fit excludes the peak point, since a branch that ends at the peak is not the branch being fitted. On that convention it gives a bare-to-dowelled ratio of 2.47 against 2.24 for the secant, and a step in composite action of 4.8 to 9.2 percentage points rather than the 5.8 to 9.7 reported here. Retaining the peak would drop the two group means to 0.365 and 0.817 and bring the ratio back to 2.24, so the exclusion is what makes the two estimators distinguishable. Every point on the record is eligible for the secant, including the first: the grid has no point at zero displacement, and skipping it would silently take the second-largest value on the two specimens whose maximum falls there. Because the framework enters the slip axis only through the product (Section 7.2), a change of scale in that axis changes no prediction, which Section 7.2 demonstrates. One consequence is that and are reported as step indices throughout, and the slip values of Table 4 are read as ordinates of the recorded curves rather than as displacements in millimetres.

### *4.3. What the eight specimens settle, and what they leave open*

The eight specimens allow three comparisons: surface preparation, interface reinforcement and substrate grade.

Roughening is the only comparison in which every other variable is held constant, so it is the only one the eight specimens settle on their own. LI-2, chiselled, against LI-1, wire brushed, on the same C30 substrate with no dowels: roughening raises the cracking load by 3.9 per cent, from 127.0 to 132.0 kN, and the failure load by 17.0 per cent, from 124.6 to 145.8 kN. It is better on both counts at once. The mechanism is visible in the failure modes of Section 4.1: roughening acts from the treated surface inward, so it enlarges the area over which interlock develops before the matrix cracks and delays the cracks that precede bond failure. The ascending stiffness rises with it, from 0.569 to 0.632 MPa per grid step.

Dowelling costs at one end what it buys at the other. LI-3 adds 0.94 per cent dowels to the LI-1 substrate. Peak shear stress rises from 2.49 to 5.03 MPa and the ascending stiffness from 0.569 to 1.270 MPa per grid step. The cracking load, however, falls from

127.0 to 43.0 kN, a drop of 66 per cent, while the failure load rises from 124.6 to 241.5 kN, a rise of 94 per cent. Whether that is a good trade depends on the limit state being checked, not on the material; it is a design question rather than a materials one.

The group means make the same point. The dowelled group has 2.24 times the ascending stiffness of the bare group, 1.346 against 0.600 MPa per grid step. Dowels interrupt the crack path and act only after the matrix has cracked, so one might expect them to soften the ascending branch. They stiffen it, while raising the peak by a factor of 2.02 and removing the pre-cracking reserve. The failure modes explain why: the bare joint carries almost nothing beyond cracking, so its ascending branch ends early, whereas the dowelled joint keeps loading through the matrix long after the bare one has failed.

Substrate grade can be put in order by the four constant-dowelling specimens. At 0.94 per cent dowelling, LI-3, LI-6, LI-7 and LI-8 give peak shear stresses of 5.028, 5.230, 5.008 and 5.290 MPa for C30, C40, C50 and C60. The range is 5.5 per cent of the mean and the sequence is not monotone, C50 falling below both C40 and C60, so across the C30 to C60 range the grade moves the peak by less than the scatter of four specimens and no threshold grade can be located in that range. The contrast with treatment is direct: bare against dowelled moves the peak by a factor of 2.02, while the whole C30 to C60 range moves it by 5.5 per cent. The design values of Table 4 are therefore set by treatment group, and the grade enters them only through the choice of group.

The wider sweep from which these four specimens come reports two further results, both from [10] and neither reproduced here: that beyond a substrate strength of about C50 the interface reinforcement ratio rather than the concrete strength becomes controlling, and that peak shear strength rises and then falls with the ratio, to an optimum at 1.57 per cent. Our three specimens at constant treatment and grade, LI-3, LI-4 and LI-5, give 5.028, 5.120 and 5.280 MPa at ratios of 0.94, 1.25 and 1.57 per cent. That is monotone over the range tested, so it neither confirms nor contradicts the reported optimum. The optimum is cited as a result of the wider sweep and is not used anywhere in this paper.

### *4.4. Implications for the analytical model*

Taken together, the three trends say how the interface should enter a model. A single cohesion parameter at the peak strength, which is the usual simplification, misrepresents any reinforced joint at working load, because it assigns a stiffness that the ascending branch of the measured curves shows to be considerably lower. A traction-separation law carrying both quantities takes the form

$$\tau = \frac{\tau_p}{s_p} s, \ 0 \le s \le s_p \quad (2)$$

$$\tau = \tau_p + \left(\tau_{res} - \tau_p\right) \frac{s - s_p}{s_{ult} - s_p}, \ s_p < s \le s_{ult} \quad (3)$$

Equation (3) is written to show the shape of a complete interface law; it is not evaluated anywhere in the paper, for a reason that comes from the record rather than from choice. The slip at the peak was recorded at 5 to 9 grid steps, while the slip capacity adopted for the framework is 0.40 on an intact joint and 0.20 on a precracked one, so the domain  < s <=  is empty for every specimen and its denominator is negative. The two quantities are not of the same kind, and the asymmetry matters:  is read off the recorded curve, whereas  is adopted, and Section 7.2.1 shows that the whole distance between a conservative envelope and an exact reproduction of the measured capacities lies

between those two numbers. The framework of Section 7 therefore uses only the ascending branch, through the single-valued stiffness , and the single-valued slip capacity . The residual plateau is reported in Table 4, and no prediction here depends on it.

Under repeated or reversing load the friction term has to be written explicitly, through the normal stress maintained on the interface, as

$$\tau = \tau_{coh} + \mu\sigma_n \quad (4)$$

Section 2.3 then follows: is the clamp left by the prestress, quantified in Section 6.4, and in a precracked member that is not retensioned it is taken as zero. One friction coefficient is adopted for every clamped joint, = 0.70, inside the 0.5 to 0.8 range reported for direct shear on a normal-strength substrate under a UHPC overlay [26]. It belongs to the substrate surface rather than to the treatment, and the dowels contribute interlock, which sits in the ascending stiffness rather than in the friction term. Section 6.4 checks that choice in both states and finds that it changes nothing, because the connection degree has already reached unity in each.

# 5. Analytical model

## *5.1. Basis and idealisation*

The girders and the strengthened beams were both modelled by strain compatibility on the composite section, with the interface handled separately by the two checks of Section 7.2. The model assumes plane sections, takes the neutral axis from the properties in Table 1 and Section 3.2, and obtains the moment from equilibrium between the compression block and the tensile resultants of the UHPC layer, the steel and the strand. The compression block is integrated over the real geometry, a T of 200 x 60 mm flange over an 80 x 190 mm web rather than a rectangle, and the neutral axis is located by sweeping the extreme compressive strain and solving axial equilibrium for the depth of the resultant at each step. Because the UHPC layer is cast against the soffit, the compressive strength steps from 135.53 MPa below y = to 33.63 MPa above it; in the monolithic group L4 the layer occupies the full depth and the step falls outside the section.

In tension the UHPC is elastic to the measured direct tensile strength of 11.62 MPa and then descends linearly to a residual of 0.62 of that value, which is what gives a fibre-reinforced layer a post-cracking reserve instead of a brittle loss, and what the design recommendations handle through a fibre orientation factor applied to the composite tensile strength [6,25]. The strand is capped at its yield strength of 1820 MPa; Section 6.3 shows it reaching yield in every member before the section does, so the design value of 0.87 would understate the compression the joint carries. Properties that were not measured are adopted at the values in Table 1 and flagged there. The interface enters through Equations (7) to (12) rather than through the section kinematics, so the two can be varied independently, which is what makes the comparison in Section 6.2 possible. Figure 5a shows the resulting strain state on the true geometry.

Capacity is defined at first yield of the tension reinforcement: the strand at 1820 MPa for the prestressed sections, the corroded bar at its reduced yield strength for the strengthened ones. Two other definitions were tried first. The largest moment the section could reach, found by sweeping the extreme compressive strain, is unreliable here: the tensile law of the layer descends to a residual plateau and stays flat, so the moment of a section with a yielded strand rises towards an asymptote and the largest value found is simply the last strain the sweep reached. First yield is also the state the load cells recorded, so computed and measured capacities are compared on the same footing. The material parameters are those of Table 1 and Section 3.2, as in the companion work [19].

## *5.2 The interface representation and why it changes the answer*

The companion models [19] represented the interface by a tie constraint, that is, as perfectly bonded. That is the usual simplification and it is adequate for global quantities when the joint is strong, but it cannot answer the present question: a tie makes slip identically zero and so removes the quantity whose influence is being examined.

The interface is therefore rewritten as two explicit checks, a shear flow capacity check and a slip capacity check, Equations (7) to (12) of Section 7.2. The shear flow the section demands is the tension in the UHPC layer divided by the length over which that tension builds up, which is the shear span and not the constant moment zone, since the shear force is zero there and the joint transfers nothing. The tension comes from the section analysis rather than from a reduced stress block, and only the UHPC layer contributes to it, because the bars and the tendon are anchored inside the section and never cross the joint. In the precracked state of Section 6.4 the layer tension is 28.8 kN, a demand of 48.0 N/mm across the 80 mm joint against a capacity of 216.3 N/mm, which gives an action factor of 0.5768. Figure 5b sets the two idealisations side by side: a rigid tie reports zero slip by construction and therefore cannot report a loss of composite action at all, whereas the two checks return one.

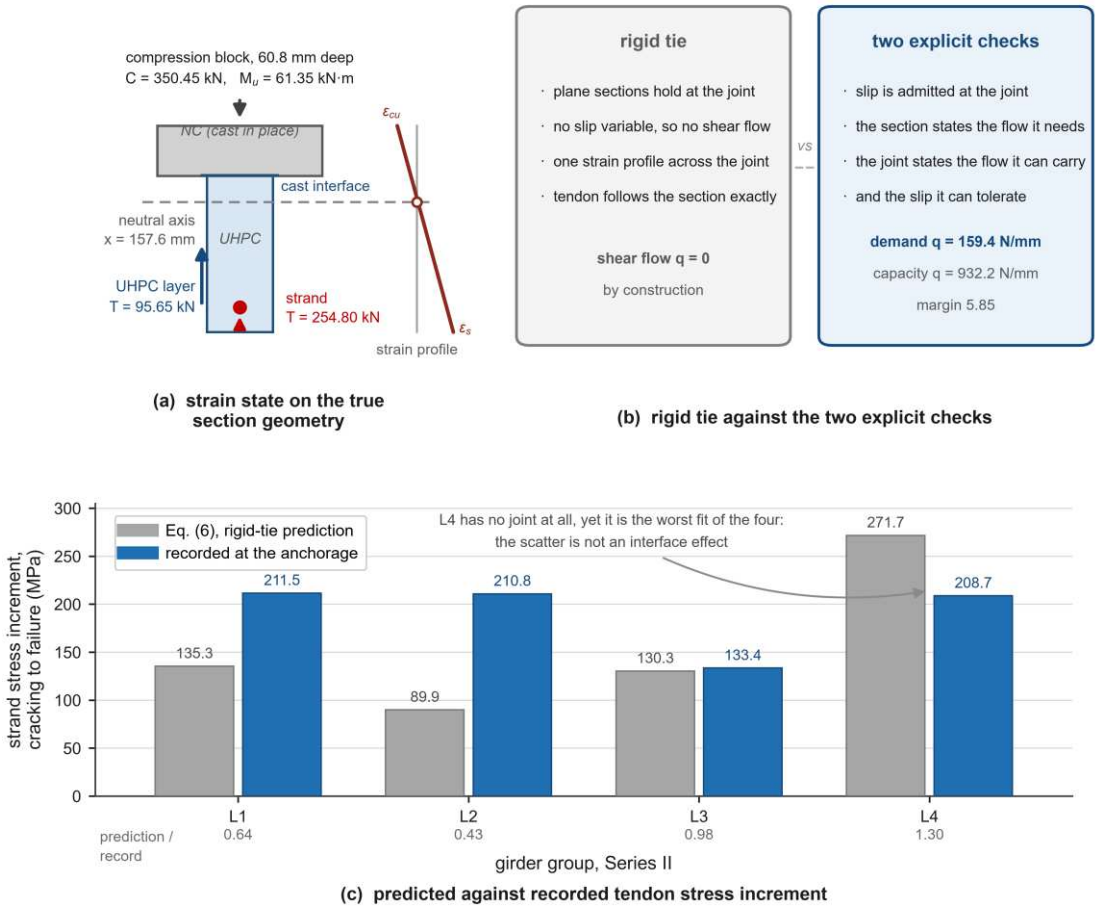



**Figure 5.** The two analytical idealisations of the interface and their consequences

### *5.3 Validation against Series II*

The reformulated models were checked against the eight girders before being used for anything else. The comparison covers cracking load, ultimate load, midspan deflection at ultimate and the tendon force recorded at the load cell. Table 5 gives the results.

**Table5.** Validation of the section-analysis model against the prestressed girders of Series II

| Girder group | (mm) | (mm) | x (mm) | (kN.m) | (kN.m) | interaction (kN.m) | Error, tie (%) | Test / full interaction | (N/mm) | (N/mm) |
|---|---|---|---|---|---|---|---|---|---|---|
| L1 | 160 | 90 | 155.7 | 74.88 | 61.32 | 70.97 | −5.23 | 1.055 | 157.5 | 932.2 |
| L2 | 190 | 60 | 157.6 | 77.10 | 61.35 | 71.01 | −7.90 | 1.086 | 159.4 | 932.2 |
| L3 | 220 | 30 | 180.4 | 79.04 | 63.95 | 74.02 | −6.36 | 1.068 | 182.8 | 932.2 |
| L4 | 250 | 0 | 207.5 | 81.89 | 70.76 | 81.89 | +0.00 | 1.000 | not applicable | not applicable |

Group L4 is monolithic UHPC with no substrate and therefore no interface, so no interface check applies to it and the table reports it as not applicable rather than as zero. Its error is zero by construction, because the constant K is set by matching it, and the other three errors are measured against that match. The model under-predicts all three interface-bearing groups by 5.2 to 7.9 per cent. That common sign is arithmetic, not evidence: with a single constant anchored on one group, the sign of the residual follows from the choice of anchor, and anchoring on L4 gives three negative errors where anchoring on L2 gives three positive ones, +2.9, +1.7 and +8.6 per cent. The sign therefore carries no statistical meaning. What the comparison does establish is the size of the misfit, 5.2 to 7.9 per cent across three groups spanning three layer depths and two substrate grades, and the fact that one constant covers all three without a trend in the residual. Section 7.3 reports the consequence rather than correcting for it here. The measured backbone is close to linear in layer depth, Mu = 62.53 + 0.0766 in kN.m, with a coefficient of determination of 0.994 over four groups.

The neutral axis does not stay put as the layer deepens. It rises from 155.7 mm at = 160 mm to 157.6, 180.4 and 207.5 mm at = 190, 220 and 250 mm, and the compression block falls from 62.7 mm to 60.8, 38.4 and 16.5 mm. Every millimetre of UHPC added in the tension zone moves the compression resultant upward, because more of the tensile resultant is carried at a lower level. The three interface-bearing groups therefore differ in their compression blocks as well as in their layer depths, and none is a scaled copy of another. Figure 6 shows the strain fields of the two girders that bracket that range.

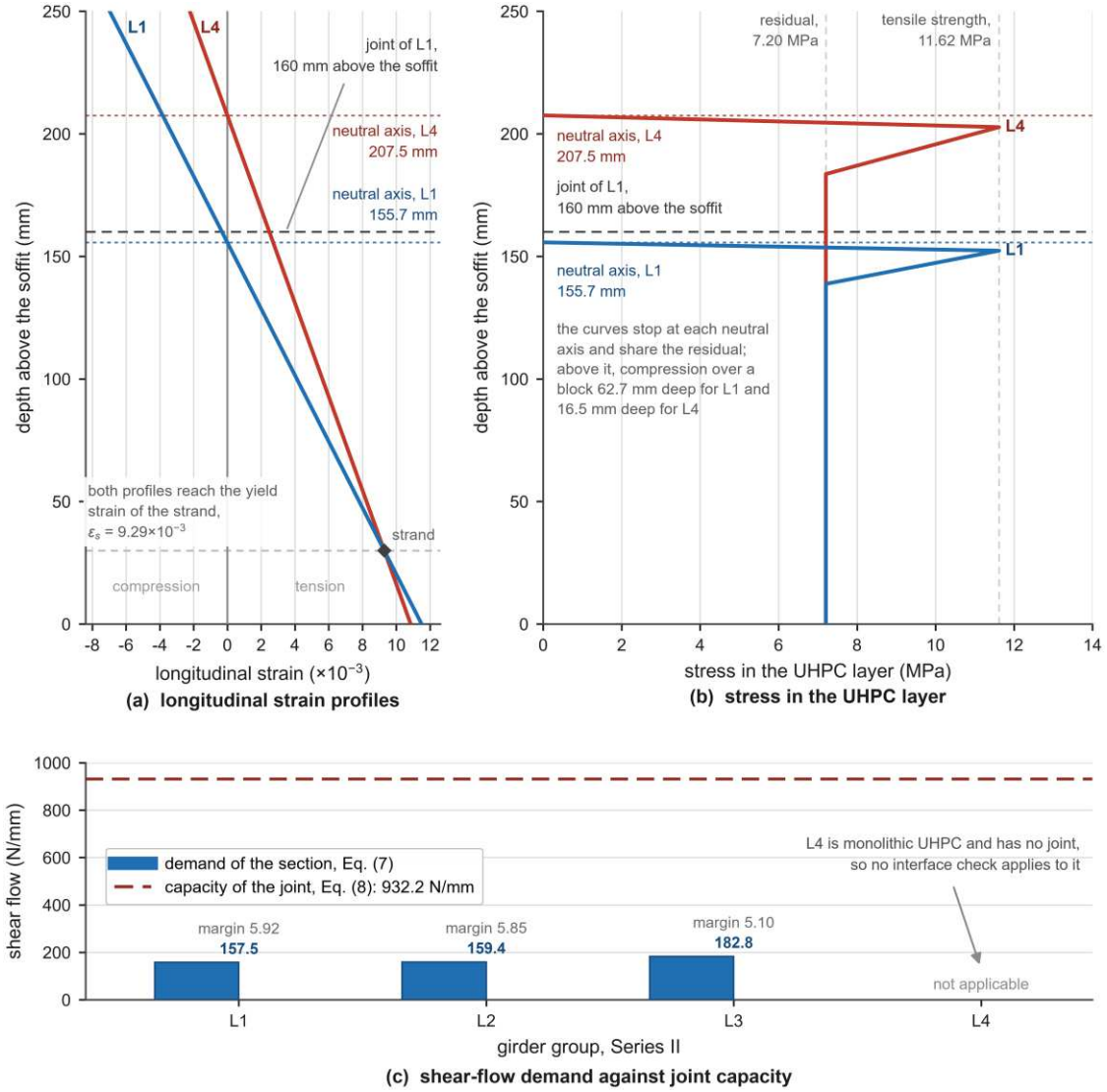



**Figure 6.** Maximum principal strain fields of the two girders that bracket the interface question, from the analysis of Section 5.1

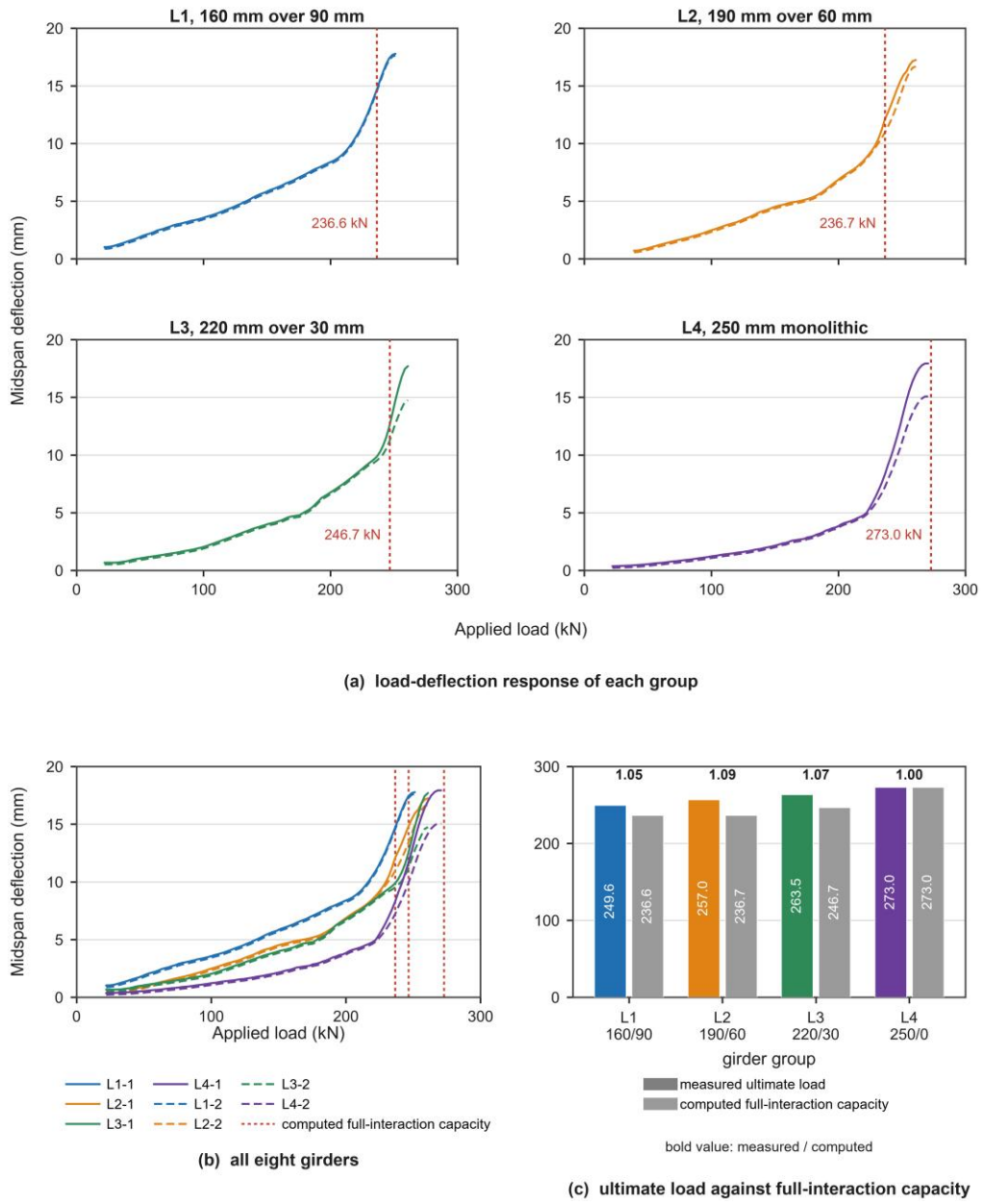



**Figure 7.** Load-deflection response of the eight prestressed girders, at midspan of the 1800 mm span

The tie model reproduces the ultimate load of the monolithic group exactly and under-predicts the three interface-bearing groups by no more than 7.9 per cent, so for global quantities the choice of interface representation hardly matters. It does not follow that the joint can be ignored. What a tie cannot represent is the tendon force history: a rigid interface implies full compatibility and therefore strains the tendon more than a joint that can slip. Section 6.3 quantifies the difference and finds it common to all four groups, including the one with no joint, which puts its origin in the elastic assumption rather than in the interface. Figure 7 gives the measured load-deflection response and marks the load at which the computed full-interaction capacity of each group is reached.

### *5.4 Validation against Series III*

The interface models were then checked against the ten strengthened beams, using the parameters appropriate to the treatment of each. All ten failed in a ductile manner with no measurable interface slip. Table 6 reports the comparison, and Figure 8 arranges the beams as the four parameter sweeps they form.

These beams are plain reinforced concrete and carry no tendon, so the section analysis contains no prestressing term. That matters quantitatively rather than formally: the 140 mm2 of strand used in Series II would add 254.8 kN to a tensile resultant of about 490 kN in a 250 mm section, more than half of the whole.

**Table 6.** Validation of the section-analysis model against the service-damaged strengthened beams of Series III.

| Beam | Corrosion (%) | (mm) | (kN.m) | (kN.m) | Error (%) | Test / model |
|---|---|---|---|---|---|---|
| L1 | 0 | 50 | 60.15 | 58.04 | −3.51 | 1.036 |
| L2 | 3 | 50 | 56.10 | 55.42 | −1.21 | 1.012 |
| L3 | 8 | 50 | 51.15 | 51.15 | +0.00 | 1.000 |
| L4 | 13 | 50 | 47.85 | 47.00 | −1.78 | 1.018 |
| L5 | 8 | 60 | 53.70 | 52.24 | −2.72 | 1.028 |
| L6 | 8 | 70 | 52.35 | 53.25 | +1.72 | 0.983 |
| L7 | 8 | 50 | 41.25 | 41.21 | −0.09 | 1.001 |
| L8 | 8 | 50 | 62.40 | 60.66 | −2.79 | 1.029 |
| L9 | 8 | 50 | 49.50 | 51.15 | +3.33 | 0.968 |
| L10 | 8 | 50 | 50.70 | 51.15 | +0.89 | 0.991 |

The scatter about the anchor is a root mean square of 2.17 per cent over all ten errors, with a mean error of -0.62 per cent, a standard deviation of 2.19 points on the divisor n - 1, and a range of 6.84 points. Six of the ten errors are negative, three positive and one zero. Because the error at L3 is zero by construction rather than by agreement, only nine residuals are free, and the root mean square over those nine is 2.28 per cent; that is the figure to quote when judging the reproduction. Throughout the paper a standard deviation uses the divisor n - 1, a root mean square uses the free residuals, and 95 per cent intervals use Student t on n - 1 degrees of freedom. One anchored constant therefore spans four independent parameter sweeps to within 2.28 per cent, and since the anchor is itself a fitted member, Section 7.3 treats the result as a reproduction rather than as a prediction.

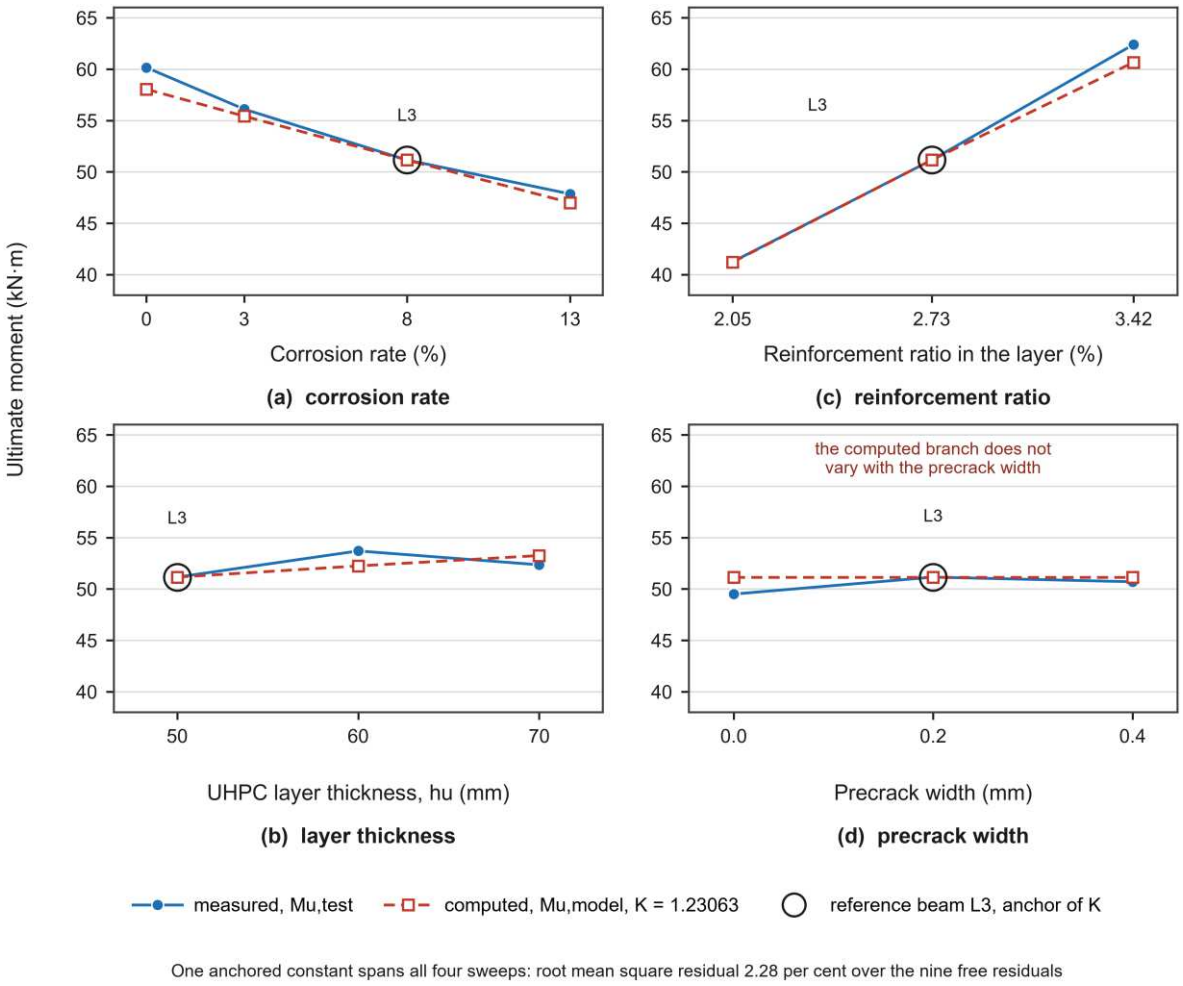



**Figure 8.** The ten strengthened beams, arranged as the four parameter sweeps they form about the reference beam L3

## 6. Mechanism analysis

### *6.1 What governs the action factor, and what does not*

Section 4 separated the bare and dowelled joints by a factor of 2.02 in peak shear stress and 2.24 in measured ascending stiffness. Whether either difference survives into the flexural capacity of a girder is a separate question. This section answers it by putting every measured specimen on one common section, which Figure 9 does for all eight.

Take the section of girder L2, whose joint demands 159.4 N/mm, and evaluate all eight specimens on it with one protocol: the slip capacity of an intact joint, 0.40, for every specimen alike. Fixing that quantity is what makes the eight comparable, so any difference below belongs to the treatment and to nothing else. The precracked value of 0.20 is a different state and is applied in Section 6.4.

Under that protocol the connection degree is unity for all eight, and the action factor runs from 0.5315 and 0.5382 for the two bare specimens to between 0.5957 and 0.6286 for the six dowelled ones. The step from bare to dowelled is worth 5.8 to 9.7 percentage points, and it comes from the ascending stiffness: across the six dowelled specimens the peak shear stress varies by 5.5 per cent on the range-to-mean measure used here, the stiffness varies by a factor of 1.26, and the action factor moves 3.3 points with it. With the strength check at unity throughout, all of that movement is the slip-flow capacity of Equation (13) and none of it is cohesion.

Cohesion on its own does not move the answer, and the strength margins show why. The dowelled joint carries 932.2 N/mm against a demand of 159.4 N/mm, a factor of 5.85;

on the bare section of a strengthened beam the capacity is 216.3 N/mm against 48.0 N/mm, a factor of 4.50; and the smallest margin among the sixteen parameter cases is 1.36, on the L2 section with bare parameters and no clamp. Section 6.4 shows that no tested member is in that state, and that the weakest member actually tested passes by 3.22. A check that never closes cannot govern, and setting cohesion to zero on the clamped section still leaves 519.4 N/mm and a margin of 3.26. What decides the answer is the slip capacity and the ascending stiffness together, through the product of Section 7.2.

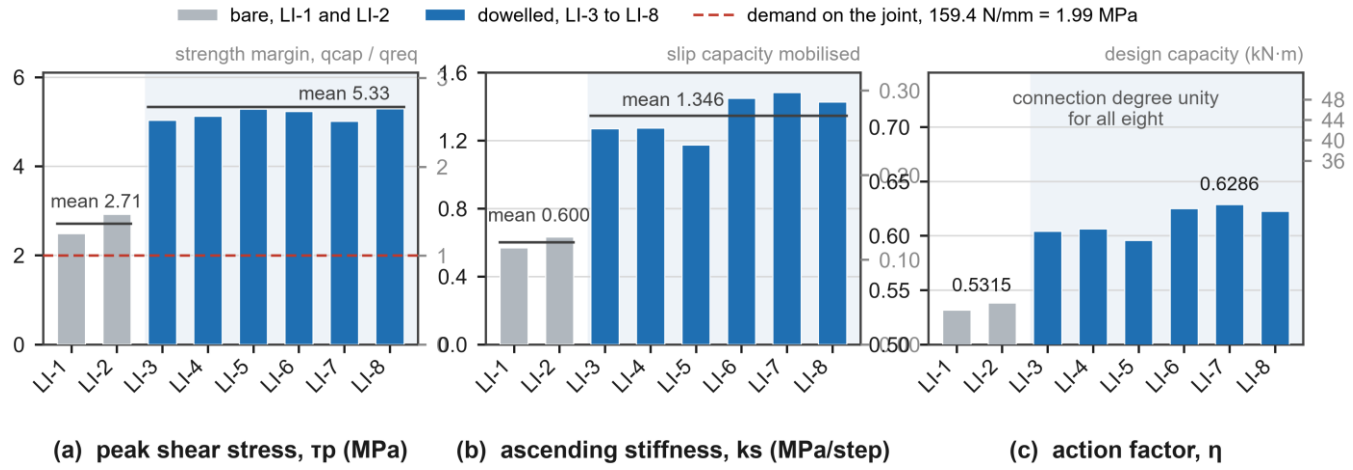



**Figure 9.** The eight measured interface specimens evaluated on one common section, girder L2, whose joint demands 159.4 N/mm, and under one protocol, the slip capacity of an intact joint

*6.2 What each treatment buys, in the limit state it affects*

The two treatments cannot be ranked, because they act in different limit states. Roughening improves both ends: LI-2 against LI-1 raises the cracking load by 3.9 per cent and the failure load by 17.0 per cent, and there is no regime in which the wire-brushed joint is the better choice, which makes roughening the default for a substrate that is sound at casting. Dowelling trades one end for the other: 0.94 per cent dowels cut the cracking load by 66 per cent and raise the failure load by 94 per cent, so a girder governed by serviceability gets worse and one governed by ultimate capacity gets considerably better. Both follow from the failure modes of Section 4.1, where the dowel interrupts the crack path and delays the cracks the serviceability check looks for. The question is therefore not which treatment is stronger but which limit state the member is designed for, and neither the treatment nor the limit state appears in the parameters currently used to design this class of member.

*6.3 Prestress gain and the effect of the interface*

The load cell at the anchorage gives the total tendon force directly through the loading history. Four values are extracted: the initial force recorded immediately after tensioning, the force at cracking, the force when the section yields, and the force at failure. The prestress gain is

$$g_p = \frac{P_u - P_0}{P_0} \quad (5)$$

and the incremental stress in the tendon as = ( - )/. Figure 10 gives the recorded histories.

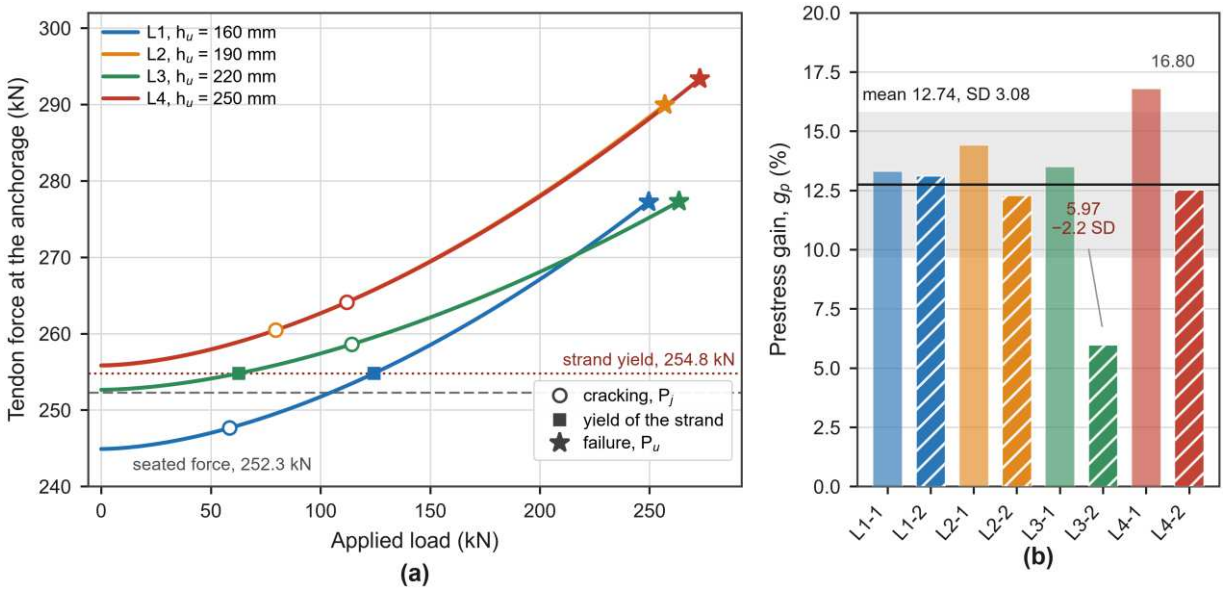



**Figure 10.** Tendon force recorded at the anchorage load cell during flexural loading, plotted against the applied load for the four girder groups, with the cracking and yield loads indicated.

The measured gains are summarised in Table 7.

**Table 7. Tendon force and prestress gain measured at the anchorage load cell, one seven-wire 15.2 mm strand of 140 mm2, Series II.**

| Girder | (mm) | P before seating (kN) | after seating (kN) | at cracking (kN) | at failure (kN) | dP (kN) | at failure (MPa) | at failure (%) |
|---|---|---|---|---|---|---|---|---|
| L1-1 | 160 | 279.7 | 243.5 | 245.0 | 275.9 | 32.4 | 231.4 | 13.31 |
| L1-2 | 160 | 288.4 | 246.3 | 250.3 | 278.6 | 32.3 | 230.7 | 13.11 |
| L2-1 | 190 | 295.6 | 255.2 | 259.1 | 292.0 | 36.8 | 262.9 | 14.42 |
| L2-2 | 190 | 294.6 | 256.4 | 261.8 | 287.9 | 31.5 | 225.0 | 12.29 |
| L3-1 | 220 | 288.8 | 254.1 | 262.9 | 288.4 | 34.3 | 245.0 | 13.50 |
| L3-2 | 220 | 293.3 | 251.2 | 254.3 | 266.2 | 15.0 | 107.1 | 5.97 |
| L4-1 | 250 | 296.7 | 255.4 | 267.0 | 298.3 | 42.9 | 306.4 | 16.80 |
| L4-2 | 250 | 289.5 | 256.3 | 261.2 | 288.4 | 32.1 | 229.3 | 12.52 |
| Mean of 8 girders | -- | 290.8 | 252.3 | 257.70 | 284.46 | 32.16 | 229.72 | 12.74 |

The tendon stress, not the increment, decides the yield question. Over the 28 days between tensioning and transfer the force falls from 290.8 to 252.3 kN, a loss of 13.2 per cent, which is creep, shrinkage and anchorage set in the substrate. On 140 mm2 of strand that seated force is 1739 to 1831 MPa, a mean of 1802 MPa and 99.0 per cent of the 1820 MPa yield strength, so the tendon is at yield from transfer and not only at the end of the test. The tensioning value itself is 2077 MPa on the same area, 114 per cent of yield, so the strand was yielded at tensioning and held there. At failure the cell reads 1901 to 2131 MPa, a mean of 2032 MPa or 111.6 per cent of yield, which is 2.9 per cent above the 1975 MPa ultimate strength: a strand that did not fracture cannot sustain that, so the reading is treated as an upper bound rather than a stress the material reaches. The analysis uses the

yield strength throughout, and the increment between seating and failure is a post-yield quantity, not a stiffness.

Figure 5c sets that increment against the value the tie model returns. Under full interaction the section that develops the moment also stretches the tendon, so the increment follows from the moment carried between cracking and failure acting on the lever arm of the strand,

$$\sigma_{p,inc} = \frac{E_p}{E_u}\left(M_{u,full} - M_j\right)\frac{z_p}{I_g} \quad (6)$$

where is the modulus of the UHPC, the moment at which the extreme tensile fibre reaches its direct tensile strength with the prestress already present, and the second moment of area of the transformed section at that state. Equation (6) is elastic and applies to the uncracked section, which is why the modular ratio is written out: the factor / converts a stress read on the section transformed to UHPC units into a stress in the strand.

Equation (6) returns increments of 135.3, 89.9, 130.3 and 271.7 MPa for L1 to L4. The measured counterpart is the increment between cracking and failure, ( − )/, which the record gives as 211.5, 210.8, 133.4 and 208.7 MPa. The ratio of prediction to measurement is therefore 0.640, 0.426, 0.976 and 1.302. These are not the increments of Table 7, which start at seating and include the pre-cracking part of the history; they are different intervals over the same record and are kept separate here.

The relation is close for L3 and off by a factor of 2.3 for L2, and the departure is not an interface effect. Group L4 has no joint at all, so slip cannot explain it, and its ratio of 1.302 is the furthest from unity of the four. What the comparison shows is that an elastic lever-arm relation on the uncracked section cannot represent a tendon that was already at yield when the increment began: with the seated stress at 1802 MPa, or 99.0 per cent of yield, the tendon responds on a post-yield tangent rather than on from the first load step, so the relation overstates the increment for the three groups that yield early and understates it for the one that does not. Equation (6) does not measure the interface; the four ratios scatter about unity rather than about any single offset.

The gain itself is 12.74 per cent of the seated force, with a standard deviation of 3.08 on the divisor n - 1, a coefficient of variation of 24.2 per cent, a median of 13.21 and a range of 5.97 to 16.80. The 95 per cent confidence interval on the mean, from Student t on seven degrees of freedom, is 10.17 to 15.31 per cent. Girder L3-2, at 5.97 per cent, lies 2.20 standard deviations below the mean and is the one specimen that looks different from the rest; it is retained in every table here, and the interval quoted with it is the one that includes it. Leaving it out gives a mean of 13.71 per cent and a standard deviation of 1.53 over seven girders. In absolute terms the mean increment is 32.2 kN with a standard deviation of 7.9 kN. Within each pair the spread is of the same order as the difference between groups, which is worth remembering when reading the group means of Table 2.

The cell reads at the girder end, so it understates the tendon force at midspan, where the strand has already yielded at failure. The tabulated gains are therefore lower bounds.

### *6.4 The same interface in a clamped and an unclamped state*

The prestressed girders and the strengthened beams differ in one respect that matters: the prestressed section carries a permanent normal compression across its joint and the strengthened one does not. The seated force of 252.3 kN acting on the 27200 mm2 gross section puts 9.276 MPa of uniform compression on the joint, a quantity unrelated to the 1802 MPa tendon stress. At a friction coefficient of 0.70 that mobilises 6.49 MPa, more than the cohesion of any of the eight specimens, which ranges from 2.49 to 5.29 MPa. Friction is therefore 55.7 per cent of the capacity of the clamped joint, and the strength check below is a check on a capacity that is more than half friction.

None of that changes the result. Take the L2 section, whose joint demands 159.4 N/mm, and hold the treatment fixed while the clamp is removed and restored. Dowelled and clamped, the capacity is 932.2 N/mm and the check passes by 5.85; dowelled and unclamped, 412.7 N/mm and 2.59; bare and clamped, 735.8 N/mm and 4.62; bare and unclamped, 216.3 N/mm and 1.36. The connection degree is unity in all four, as it is in every one of the sixteen parameter cases of Section 6.1. Setting cohesion to zero and leaving friction alone still leaves a margin of 3.26. Figure 11 shows the four states side by side.

The margin of 1.36 is the smallest of the sixteen cases, and it should be read for what it is. It is not the margin of a specimen: it is a bare, unclamped joint, which no specimen in either series was tested with, imposed on the L2 section, whose 159.4 N/mm demand belongs to the Series II girders. No tested member combines the two. Among the sixteen members that carry a joint, the margins are 5.92, 5.85 and 5.10 on the three Series II groups. On the Series III beams, where there is no tendon and the substrate was cracked before the layer was cast so the joint compression is zero, the demand is 48.0 N/mm at eight of the ten and rises with layer thickness to 67.2 N/mm at the 70 mm layer of L6, against a bare-joint capacity of 216.3 N/mm throughout; that gives 4.50 for those eight and 3.22 for L6. The smallest margin among the members actually tested is therefore 3.22.

The distinction cuts against the framework rather than for it. The synthetic case that produces 1.36 puts the most demanding section together with the weakest joint and no clamp, and it still passes; the real members pass by more. A check that cannot close at 1.36 cannot govern, and neither can one that cannot close at 3.22.

The clamp is therefore worth nothing through friction, because the friction is never the binding term. What it is worth is the doubling of slip capacity that compression across the plane makes available, from 0.20 on a precracked joint to 0.40 on an intact one, and that enters through the same product as the ascending stiffness. On the L2 section, restoring the clamp multiplies the action factor of a precracked bare joint by 1.063, from 0.5029 to 0.5348, and on a sound dowelled joint by exactly 1.000, because there the slip capacity is already 0.40 and the clamp changes only a capacity the strength check did not need. The clamp and the interface stiffness are not two findings: both act on through the slip-flow capacity of Equation (13) alone, and their ratio of 4.48 in that capacity is the whole of the difference between them.

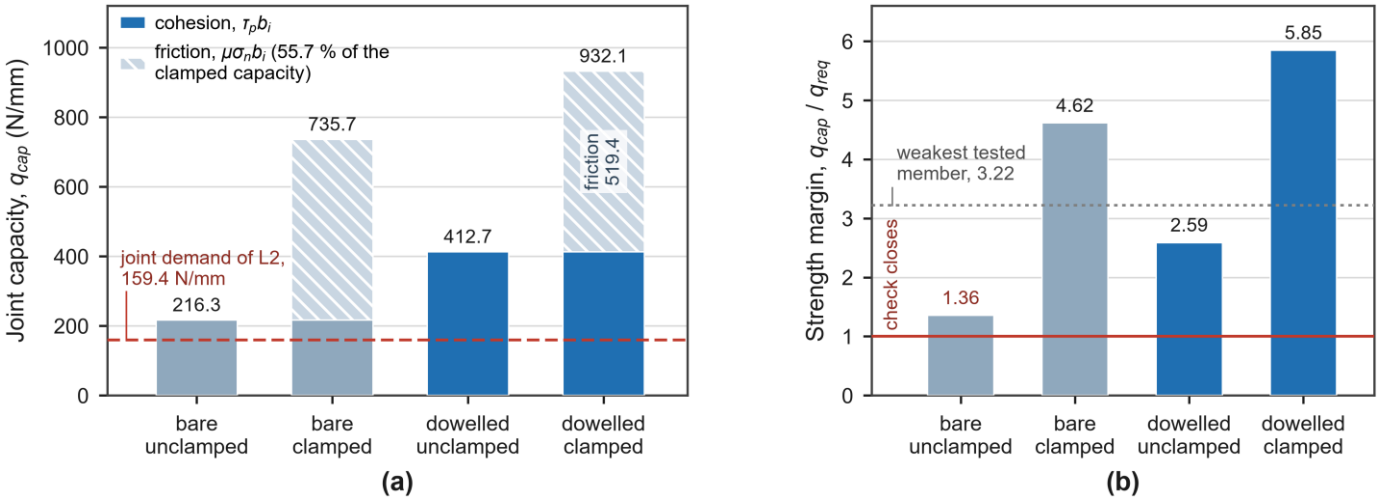



**Figure 11.** The same interface in four states, all evaluated on the section of girder L2

## 7. A conservative assessment of the bond-based check

### *7.1 Full-interaction reference capacity*

A fully interactive section is analysed in the conventional way: plane sections, the neutral axis from axial equilibrium of the compression block against the tension in the steel, the tendon and the UHPC layer, and the moment taken about the compression resultant. For these sections the analysis is that of Section 5.1 and the results are in Table 5. One constant enters it, and it is the only constant in the prestressed series that is not measured.

Group L4 is 250 mm of UHPC with no substrate, so its connection degree is unity by definition and its measured capacity of 81.89 kN.m fixes the fully interactive capacity of that section at 70.76 kN.m. The ratio, K = 1.15736, scales the computed capacity. Applied to the three groups that have a joint it under-predicts their measured capacities by 5.2 to 7.9 per cent, all on the conservative side, and that sets the accuracy of the assessment in Section 7.3.

The constant multiplies the moment of the whole section rather than the UHPC contribution alone. Equation (1) explains why: the action factor is a ratio of two section moments, so it scales the section capacity and not one term of the equilibrium. For the strengthened series of Section 5.4 the same form applies with K = 1.23063, anchored on group L3. The two anchors differ by 6.3 per cent, which is the difference between a section with a tendon and one without.

The equivalent rectangular stress block of over , the usual closed-form way of writing the UHPC contribution, is not used. It assumes a uniform tensile stress over the layer depth, which for a layer whose stress varies with depth and whose post-cracking capacity is a residual rather than a plateau understates the contribution badly. Every UHPC tension in this paper comes from the section analysis.

### *7.2 Two limit states on the joint, and the one that governs*

The joint is checked twice: once for the shear flow it can carry, and once for the slip it can accommodate before the strength it has is mobilised.

The first check is strength. The section demands a shear flow equal to the tension the UHPC layer develops divided by the length over which it develops it,

$$q_{req} = \frac{T_{UHPC}}{a} \quad (7)$$

where a is the shear span, 600 mm in these girders, since the shear force is zero over the constant moment zone and the joint transfers nothing there. The joint resists the flow over its own width, the 80 mm web and not the flange, with the cohesion of Table 4 and the friction mobilised by whatever normal compression the state provides,

$$q_{cap} = (\tau_p + \mu\sigma_n)b_i \quad (8)$$

The connection degree is their ratio, capped at unity,

$$\varphi = min\left(1, \frac{q_{cap}}{q_{req}}\right) \quad (9)$$

The second check is deformation. The same demand acting on a joint of ascending stiffness opens it by

$$d_d = \frac{q_{req}}{k_s b_i} \quad (10)$$

so the fraction of the available slip mobilised by that opening is

$$mob = min\left(1, \frac{s_{ult}}{d_d}\right) \quad (11)$$

where is the slip capacity of the joint, an adopted quantity rather than a measurement: 0.40 on the recorded grid for an intact joint and 0.20 for a precracked one. The recorded slip channel of Series I is the integer grid 1 to 10, so neither value is a point on it, and the measured peak slips of Table 4 are 5 to 9 steps, an order of magnitude above . Section 7.2.1 reports what the framework does across that gap, since it is the assumption

and not the data that keeps the framework in the regime where it discriminates. The capacity is not derived from and : setting = / would reduce Equation (11) to min(1, /), which is Equation (9) again, and the two checks would collapse into one.

The action factor combines the two,

$$\eta = \eta_0 + (1 - \eta_0)\varphi\ mob \tag{12}$$

in which = 0.4711 is the ratio of the interface-brittle peak stress of LI-1 to the interlock-dominated peak stress of LI-8, both measured in Series I. It is the composite action of the fully separated limit, taken from measurement rather than fitted. Equation (12) is unity when both checks pass and falls to when the joint cannot develop its tension at all, which is the state of a section whose layer has come away from its substrate.

The deformation check and the mobilisation ratio are written with the same three interface quantities, so one can be substituted into the other.

Substituting Equation (10) into Equation (11) gives

$$mob = min\left(1, \frac{s_{ult} k_s b_i}{q_{req}}\right) \tag{13}$$

The deformation check therefore depends on the interface only through the product of slip capacity and ascending stiffness, written here. Cohesion, friction and clamping stress enter only through Equation (9), and Section 6.4 shows at unity in all sixteen cases examined, so through that equation they do not enter at all. They are not absent from the answer, because in Equation (12) is itself a cohesion ratio, taken from the interface-brittle specimen over the interlock-dominated one. The framework is a two-parameter family in (, ), and Section 8.1 gives the sensitivity: changing the peak stress of LI-1 by 20 per cent moves between 0.377 and 0.565, and moves the action factor of a bare joint between 0.564 and 0.696 on the strengthened-beam demand and between 0.433 and 0.605 on the prestressed one. The interval depends on the section because the two terms of Equation (12) are weighted by (1 - ) and , so the same change in cohesion moves a lightly stressed section more than a heavily stressed one.

Second, is invariant under a rescaling of the slip axis. Substituting -> /L and -> L into Equation (13) leaves it unchanged, so , and are all unchanged; only changes, because it is the one quantity carrying an explicit length. The absolute scale of the recorded displacement channel, which Section 4.2 shows is not recoverable, therefore changes no prediction here. On the L2 section, sweeping L from 0.1 to 10 returns = 0.613666 in every case, a range of zero within the precision of the calculation. What the missing scale costs is comparability with an absolute value in a design code, which is a matter of calibration rather than prediction.

The invariance is a property of the algebra and says nothing about robustness. survives a rescaling of the slip axis, but is an adopted value, and that value decides which branch of Equation (13) the framework sits in. Table 8 gives the action factor over the range that matters.

**Table 8.** Action factor and its two branches over the adopted and the measured slip capacities.

| | Basis | (Series II) | (Series II) | (Series II) | (Series III) | Branch |
|---|---|---|---|---|---|---|
| 0.20 | adopted, precracked joint | 21.536 | 0.1351 | 0.5425 | 0.5768 | deformation |
| 0.40 | adopted, intact joint | 43.072 | 0.2702 | 0.6140 | 0.6825 | deformation |
| 1.0006 | = 1, strengthened section | 108.032 | 0.6776 | 0.8294 | 1.0000 | transition |

| | | | | | | |
|---|---|---|---|---|---|---|
| 1.4805 | = 1, prestressed section | 159.417 | 1.0000 | 1.0000 | 1.0000 | strength |
| 5 | smallest measured , LI-4 | 538.400 | 1.0000 | 1.0000 | 1.0000 | strength |
| 7 | median measured | 753.760 | 1.0000 | 1.0000 | 1.0000 | strength |
| 9 | largest measured , LI-1 | 969.120 | 1.0000 | 1.0000 | 1.0000 | strength |

The first implication is that the two adopted values are the only ones in the set that keep the framework in its deformation branch, which is the only branch in which Equation (13) does any work.

The critical values are = 1.0006 on the strengthened section and 1.4805 on the prestressed one, and every measured peak slip in Table 4 lies above both. On the recorded evidence the framework would never leave the deformation branch, and the action factor would be unity rather than the values reported here.

Second, the conservatism reported below follows directly from that choice. Against the strengthened beams the framework returns 0.5725 at = 0.20 and 0.9926 at = 5. The equation is the same; what separates the two is the adopted value of .

Third, the alternative reading of is not a competing account of the same numbers. A stiffness of 13.2 MPa per mm for the dowelled group is / evaluated at = 0.40, that is, the adopted assumption written back into the stiffness rather than a second measurement of it. Substituting = / into Equation (13) cancels and leaves = ; the framework then reduces to Equation (9) alone, the connection degree and the mobilisation are both unity, and Equation (12) returns = 1.0000. That reading gives 0.935 against the prestressed girders and 0.993 against the strengthened beams. It says the joint is governed by strength alone and the deformation branch does no work. The two readings are not conversions of each other: one is a measurement on the recorded grid and the other an assumption, and no rescaling of the slip axis maps a measurement onto an assumption. This paper runs the first model, retaining a deformation check whose parameters are adopted, and Table 8 reports what that costs.

A second reading, 2.6 MPa per mm for the bare group, has been withdrawn. It cannot be obtained from / at any slip capacity: the bare group gives 6.23, 7.29 and a group mean of 6.76 at = 0.40, and 2.6 was a literal in an early numerical script rather than a derived quantity. The conversion factor between the two readings for the bare group is 11.27, not the 4.33 quoted in an earlier draft, so the factors 9.83 and 4.33 were never comparable. What remains is the comparison above: the alternative reading collapses the framework to its strength branch, and the adopted values keep it in the deformation branch.

The framework is an envelope that needs member-level calibration before it could serve as a capacity estimate. Such a calibration would replace the adopted with a value identified on a recoverable displacement channel, and Table 8 shows that this substitution alone decides whether the framework reads as conservative or as exact.

### *7.3 Assessment against the measured capacity*

The expression is tested against two independent data sets: the three Series II groups that have a joint, which are clamped, and the ten Series III beams, which are not. Each prediction is the section analysis of that member scaled by the action factor of Equation (12), evaluated with the design values of Table 4 for the state of its joint. No member enters its own prediction: the Series II groups are predicted from the monolithic group L4 and the Series III beams from group L3. Figure 12 gives the comparison.

For Series II the joint is dowelled and clamped, so = 5.159 MPa and = 1.346 MPa per grid step, the means of LI-3 to LI-8, with = 0.70 and = 9.276 MPa. The strength check passes by 5.92 on L1, 5.85 on L2 and 5.10 on L3, so it governs nowhere and the prediction is set by the deformation term alone, at action factors of 0.6154, 0.6137 and 0.5954 for L1, L2 and L3. Applied to the calibrated full-interaction capacity of each group this predicts 43.67, 43.57 and 44.07 kN.m, a mean of 43.77 against a measured mean of 77.01, a ratio of 0.568. Applied to the uncalibrated analysis, the form a designer would compute because it uses no measured member, the same action factors give 37.82 kN.m and a ratio of 0.491. Group L4 is excluded because it has no joint: its action factor is unity by definition and there is nothing to predict.

For Series III the joint is bare and precracked, so = 2.704 MPa and = 0.600 MPa per grid step, the means of LI-1 and LI-2, with no clamp, which makes the friction term of Equation (4) vanish whatever coefficient is adopted, and a slip capacity of 0.20 rather than 0.40. The strength check passes throughout, by 4.50 at the eight beams where it does not vary and 3.22 at the deepest layer of L6, so again the deformation term sets the prediction. The action factor runs from 0.5466 to 0.5768 across the ten beams, following the thickness of the new layer rather than anything else, and averages 0.5720. Against the calibrated capacity this predicts a mean of 29.81 kN.m against a measured mean of 52.52 kN.m, a ratio of 0.568; the uncalibrated analysis returns 24.23 kN.m and a ratio of 0.461.

Both data sets therefore give 0.568 against the calibrated analysis and 0.46 to 0.49 against the uncalibrated one, so the framework is conservative by a factor of 1.8 to 2.2. The reason is in the structure of Equation (12): the action factor multiplies a capacity that is itself the product of a computed section analysis and a single fitted anchor, and on these members the joint never came near either limit state. That is why the result is an envelope rather than a reproduction of capacity.

A provision with no interface check computes the full-interaction capacity by definition. For Series III that unanchored capacity is 42.36 kN.m against a measured mean of 52.52 kN.m, so the ten beams exceeded it by 24.0 per cent. They did not fall short of their own full-interaction capacity, and Series III therefore contains no interface-controlled failure. All ten were ductile, with no measurable slip, and their characteristic loads fall almost monotonically with corrosion, from 401 kN at zero to 319 kN at 13 per cent, which is a substrate and section effect. Series II behaves the same way: all eight girders failed in flexure. The evidence for the interface mechanism comes from Series I, which measured it directly, and from the two-state comparison of Section 6.4, which follows from Series I. No member-level failure in this programme was controlled by the joint, so a framework written to predict such a failure cannot be validated against either member series.

One point of method remains. The reproduction model of Section 5.4 is anchored on group L3 through K = 1.23063, so agreement with that anchor is built into the comparison rather than predicted by it, and the ten beams span to a residual scatter of 2.28 per cent over the nine free residuals. The uncalibrated prediction is the one that uses no fitted member, and it returns 0.461 against the 24.0 per cent by which those beams exceeded their own unanchored capacity. The gap measures how little the interface moved these members.

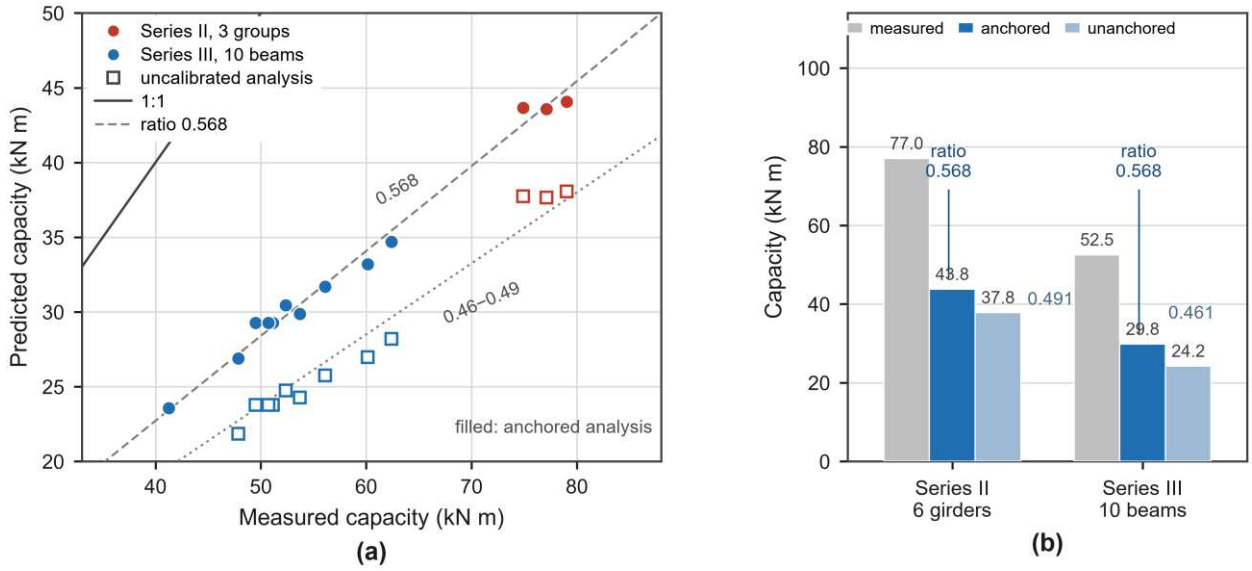



**Figure 12.**The conservative assessment against the measured capacity of the sixteen interface-bearing girders and beams, on the anchored section analysis of Section 7.1

**Table 9.** The conservative assessment against both data sets, with the two reference capacities set out separately.

| Data set | Measured (kN.m) | Uncal. analysis (kN.m) | Cal. analysis (kN.m) | Action factor, Eq. (12) | Predicted, uncal. (kN.m) | Predicted, cal. (kN.m) | Uncal. / meas. | Cal. / meas. |
|---|---|---|---|---|---|---|---|---|
| Prestressed girders, Series II, 3 groups of 2 | 77.01 | 62.21 | 72.00 | 0.595 to 0.615 | 37.82 | 43.77 | 0.491 | 0.568 |
| Strengthened beams, Series III, 10 members | 52.52 | 42.36 | 52.13 | 0.547 to 0.577 | 24.23 | 29.81 | 0.461 | 0.568 |

The two reference columns differ by the anchor of Section 7.1 and by nothing else: 1.15736 for the prestressed series, anchored on the monolithic group L4, and 1.23063 for the strengthened series, anchored on L3. The uncalibrated column needs no measured member; the calibrated one shows the expression sitting below a measured series. The calibrated prestressed capacity, 72.00 kN.m, is also the mean of the three group capacities in Table 5, 70.97, 71.01 and 74.02, as it must be, since the anchor group L4 contributes no member to the average. The measured capacity of L4, 81.89 kN.m, appears in Table 5 and in the description of Series II, but it belongs to a member without a joint and is not part of this series, so it does not enter the mean.

Two numbers in Table 9 have to be read together, because separately they say opposite things. The framework gives the strengthened beams an action factor of 0.547 to 0.577, treating them as losing between 42 and 45 per cent of the composite action their section would provide at full interaction. Those same ten beams exceed their own unanchored full-interaction capacity by 24.0 per cent, so whatever composite action the joint lost, it was not enough to take them below the capacity of the same section analysed as monolithic. Both statements come from the measurements or follow directly from them. The resolution is that the interface never became the controlling mechanism in these members, and the deformation branch, the only part of the framework that would register such a

loss, was not activated in any of them. Section 8.3 draws the consequence for how the framework should be used.

*7.4 Worked example and sensitivity*

The worked example is the section of girder L2: a 190 mm UHPC layer over a 60 mm substrate, a joint width of 80 mm equal to the web, and one tendon of 140 mm2 at a yield strength of 1820 MPa. Two of the quantities come from measurement. The seated force of 252.3 kN acting on the 27200 mm2 gross section gives a clamping stress = 9.276 MPa, and the seated stress on the 140 mm2 of strand is 1802 MPa, 99.0 per cent of yield. The two act on different areas and are different quantities, the second larger than the first by a factor of 194.

The section analysis gives a neutral axis 157.6 mm above the soffit, a compression block 60.8 mm deep, a fully interactive capacity of 61.35 kN.m and a tension of 350.45 kN, of which the tendon carries 254.80 kN and the UHPC layer 95.65 kN. The joint therefore carries 95.65 kN over the 600 mm shear span, or 159.42 N/mm. Six joints are then examined, differing only in treatment and in whether the clamp is present. The capacities below are quoted on the anchored basis of Section 7.1, that is 61.35 kN.m multiplied by 1.15736 to give 71.01 kN.m, so that they can be compared with the measured capacities of Table 9; the unanchored 61.35 kN.m is the value computed with no fitted member, and every capacity below scales from it by 1.15736.

A bare wire-brushed joint, LI-1, gives = 199.4 N/mm from cohesion alone. That exceeds the 159.42 N/mm demand, so the strength check passes and the connection degree is unity. The demand opens 3.502 steps of the grid of Table 4, which mobilises 0.114 of the 0.40 slip capacity of an intact joint and returns an action factor of 0.5315 and a design capacity of 37.74 kN.m.

Roughening the same substrate changes little. LI-2 raises to 233.3 N/mm, still above the demand, and opens 3.153 steps for an action factor of 0.5382 and a capacity of 38.21 kN.m. Restoring the clamp raises again, to 752.7 N/mm, and changes nothing else: the connection degree was already unity and stays unity, and the opening is unchanged because the clamp adds friction across the plane without altering the stiffness of the matrix that has to open. The action factor stays at 0.5382 and the capacity at 38.21 kN.m. The same holds for the bare joint, whose capacity rises from 199.4 to 718.8 N/mm with the clamp while its action factor does not move at all.

Dowelling is what moves the answer. LI-3 opens 1.590 steps for the same demand and returns an action factor of 0.6041 and a capacity of 42.90 kN.m with no clamp at all, because its ascending stiffness of 1.270 MPa per grid step is 2.20 times that of the bare group. LI-5, at 1.174, opens 1.697 steps with the clamp restored and returns 0.5957 and 42.30 kN.m. Across the six cases the design capacity varies by a factor of 1.137, the cohesion by 2.12 and the stiffness by 2.20: the capacity does not follow the cohesion, and it does follow the stiffness.

Two things raise the demand on a joint, and neither is the treatment. One is the depth of the new layer, which raises the tension it has to develop over the same shear span and took the demand across the ten strengthened beams from 48.0 N/mm at the thinnest to 67.2 N/mm at the thickest. The other is the absence of the clamp, which doubles the slip capacity available on a precracked joint and is worth a multiplier of 1.063 on this section, from 0.5029 to 0.5348 on a bare joint and exactly 1.000 on a dowelled one. Both enter through the slip-flow capacity of Equation (13) and through nothing else, which is why the clamp and the treatment produce changes of the same kind and cannot be treated as independent design variables.

## 8. Discussion

*8.1. What the framework changes*

The framework does not change the peak strength, and that is the first thing to say about it. Across every case examined here the connection degree is unity and the smallest strength margin is 1.36, so the joint capacity never controls the answer: cohesion, friction coefficient and clamping stress could each be varied over their plausible range without moving the result through that check. They are not irrelevant to the action factor. in Equation (12) is the cohesion ratio (LI-1)/(LI-8) = 0.4711, and changing the peak stress of the brittle joint by 20 per cent moves between 0.377 and 0.565, which moves the action factor of a bare joint between 0.564 and 0.696 on the strengthened-beam demand and between 0.433 and 0.605 on the prestressed one. That sensitivity, however, sits in the deformation term, and the deformation term is multiplied by a connection degree that is already one.

What does control the answer is the product of slip capacity and ascending stiffness, Equation (13), and no current interface specification carries such a product. A designer who knows only the peak strength cannot locate the answer, and the gap between the two bare and the six dowelled specimens on the same section is 5.8 to 9.7 percentage points of composite action, too large to leave unspecified. That is the practical contribution of the framework: it says which parameter has to be measured, and shows that the strength parameters do not.

The second change concerns the substrate. A joint clamped by prestress and a joint exposed on a cracked substrate differ by a factor of 4.48 in slip-flow capacity, which turns a qualitative statement about damaged substrates into a number. A specification that records the state of the substrate at casting, and the slip capacity that goes with that state, carries more useful information than one that records a bond strength.

The framework is not a capacity estimate. Against the measured series it returns 0.46 to 0.57, conservative by a factor of about two, and no member in the programme failed by interface slip against which it could be calibrated. It should be read as an envelope that shows where a bond-based check bites; design capacity should continue to come from the conventional full-interaction expression until there is member-level evidence of slip for the state in question.

*8.2. Comparison with cohesive-friction models*

The way the interface is treated here is compatible with the cohesive-friction models now common in composite girder analysis, in which a coupled cohesive-friction law represents the joint and the interface reinforcement is varied explicitly, as in the four-point bending tests and finite element models of Tong and co-workers [9] and in push-off tests on monolithically cast UHPC under combined shear and lateral load [15]. The difference is one of emphasis. Here the interface parameters are calibrated on a separate series of direct shear tests rather than back-fitted from the girder response, and the joint of interest lies between two concrete-based layers rather than inside a single monolithic section. The two approaches are complementary, and a member that combines both, such as a steel-UHPC-NC box girder, needs both calibrations. Reducing the framework to Equation (13) also says what such a model has to be given at member scale: the slip-flow capacity, that is the product of an ascending stiffness and a slip capacity in the same slip units, not a cohesion on its own.

*8.3 Limitations*

The specimens are of laboratory scale, 250 mm deep, and the size effect on the interface is not captured, so the results should not be extrapolated to full-scale girders without further work. Loading was monotonic and quasi-static, and the interface parameters were not identified under repeated loading, which is the condition that governs service in a

bridge. Corrosion in Series III was induced by an impressed current and represents uniform loss of section; localised pitting interrupts the load path over a shorter length and is more damaging at the same mass loss, so the capacities reported for that series are upper bounds [14]. The friction coefficient was adopted at 0.70 rather than measured on a clamped specimen; swept across the 0.5 to 0.8 range reported in the literature it changes the joint capacity but leaves the action factor untouched, because the connection degree is already unity with or without the clamp. The value of 0.55 that also appears in the data set for a roughened substrate was not used, for the same reason. Finally, the single constant of Section 7.1 rests on one monolithic reference member, and it under-predicts the three interface-bearing groups by 5.2 to 7.9 per cent.

The more consequential point is what the programme does not contain. The connection degree is unity everywhere, so the framework has only ever been exercised in its deformation limit, and cohesion, friction and clamping stress have never been tested at a level where they would matter. There is also no interface-controlled failure to validate against: the unanchored Series III analysis gives 42.36 kN.m against a measured mean of 52.52 kN.m, a residual of 23.9 per cent on individual members and 24.0 per cent on the mean, and the strengthened beams exceeded their unanchored capacity rather than falling short of it. Any future assessment has to begin with a member that slips.

The unrecoverable scale of the recorded slip channel is a different matter. Section 7.2 shows that the action factor depends on the slip axis only through the product , which a rescaling leaves unchanged, so no prediction here depends on recovering it. What the missing scale prevents is calibrating that product against an absolute value, which is why the framework can rank treatments and locate states but cannot yet return a capacity in code units.

### *8.4 Further work*

The first priority is a member-level test in which the joint is driven past its slip capacity, since nothing in the present programme exercises the framework where it is meant to operate. The strength check should then be exercised by widening the demand, with a longer shear span or a thinner layer, until the connection degree drops below unity and cohesion begins to matter. The direct shear tests should be repeated under maintained normal compression so that the friction coefficient is identified rather than assumed, which requires a specimen that slips while the clamp is varied. The original servo-hydraulic records should be recovered to fix the absolute scale of the slip channel. Two extensions follow from the structure of the framework: the two-state comparison of Section 6.4 relies on precracking as the only damage mechanism, and a substrate damaged by corrosion as well would separate the two effects; and the size effect on peak stress, slip at peak and ascending stiffness needs at least two further specimen scales, since the design values of Section 7.2 are otherwise tied to this one.

## 9. Conclusions

Twenty-six specimens were tested with the state of the UHPC–NC interface as the common variable: eight prestressed composite girders, eight L-shaped interface specimens and ten service-damaged strengthened beams. Twenty-four carry an interface; the two that do not are the monolithic girders L4-1 and L4-2, which leaves sixteen girders and beams with a joint. The tendon force was measured at the anchorage in every girder.

1. Bare and dowelled joints behave as different mechanisms rather than as the same mechanism at two strengths. The ratio of failure load to cracking load is 0.98 to 1.11 for the bare specimens and 5.61 to 6.01 for the dowelled ones, a factor of 5.53 between the

means, and the two ranges do not overlap. The wider sweep from which these eight specimens are drawn reports the same separation [10]; the figures here are a reduction over our subset, one specimen per condition, and are best read as a check on that result.

2. The strength check on the joint never governs. The connection degree is unity in all sixteen parameter cases, including the case with cohesion set to zero. The smallest margin is 1.36, in a combination of the most demanding section with the weakest interface and no clamp that no tested member is in; among the sixteen members tested the smallest margin is 3.22. Cohesion, friction and clamping stress therefore do not enter the action factor through Equation (9). They do enter it through , which is a cohesion ratio, so the action factor still responds to them, but through a check that never binds.

3. Substituting the slip-opening relation into the mobilisation relation leaves a single quantity, the slip-flow capacity = , and with the cohesion floor the framework is a two-parameter family. The reduction is algebra rather than a finding: any model that writes the demand as flow over stiffness and the mobilisation as slip over demand arrives at the same product, and the invariance of under a rescaling of the slip axis follows from it. What it gives the designer is something testable. The clamp and the ascending stiffness act through this one variable: restoring the clamp multiplies by 4.48 and the action factor by 1.063, and the step from bare to dowelled specimens is worth 5.8 to 9.7 percentage points of composite action, most of it from the stiffness.

4. Equation (6), an elastic relation on the uncracked section, gives 0.640, 0.426, 0.976 and 1.302 of the measured tendon stress increment for the four groups. The group with no interface is furthest from unity, so the discrepancy belongs to the elastic assumption applied to a tendon already at yield, not to the joint.

5. Dowelling and roughening cannot be ranked against each other, because they act in different limit states. Adding 0.94 per cent dowels lowers the cracking load by 66 per cent and raises the failure load by 94 per cent; roughening raises both, by 3.9 and 17.0 per cent, and is the better choice whenever the substrate is sound at the time of casting. Over the range tested the treatment governs and the substrate grade does not: peak shear stress varies by 5.5 per cent between C30 and C60 at constant dowelling, against a factor of 2.02 between treatments.

6. The prestress gain measured at the anchorage is 12.74 per cent of the seated tendon force, with a standard deviation of 3.08 over eight girders. The seated force corresponds to 1802 MPa, or 99.0 per cent of the yield strength, so the increment is a post-yield quantity rather than a stiffness. The reading becomes unreliable well below capacity, so these gains are lower bounds.

7. Against the measured capacity of both data sets the framework returns 0.568 of the clamped girders and 0.568 of the strengthened beams when the section analysis is anchored on one measured member of its own series, and 0.491 and 0.461 when it is not. No member enters its own prediction. The expression is conservative by a factor of 1.8 to 2.2, which is the 0.46 to 0.57 range quoted in the abstract.

8. No member in this programme failed by interface slip. The ten strengthened beams exceeded their own unanchored full-interaction capacity by 24.0 per cent, and all sixteen girders and beams, together with the eight L-shaped specimens, failed without measurable slip. A check meant to detect an interface-controlled failure had none to detect here, which is why it is presented as an envelope that locates where a bond-based check binds rather than as a capacity estimate.

Design of prestressed UHPC–NC composite girders therefore rests on an assumption of full interaction that held for every member tested. What the tests do not settle is where that assumption would stop holding, because no joint in the programme came close to its slip capacity. The framework indicates the condition: a joint whose slip capacity is smaller than the section demand, which in these members would require a much thinner UHPC

layer or a much longer shear span. When that case arises, the quantity a check would need is the slip-flow capacity of the joint in its state, not a bond strength. Obtaining that quantity from a member-level test rather than from a direct shear specimen remains open; the direct shear tests described in Section 4.2 are the route the literature uses [28,29].

**Author Contributions:** Conceptualization, Y.T. and J.H.; methodology, Y.T.; software, J.H.; validation, Y.T. and J.H.; formal analysis, Y.T.; investigation, Y.T.; resources, Y.T.; data curation, J.H.; writing—original draft preparation, Y.T.; writing—review and editing, J.H.; visualization, J.H.; supervision, Y.T.; project administration, Y.T.; funding acquisition, Y.T. All authors have read and agreed to the published version of the manuscript.

**Funding:** This research was funded by the following projects: (1) the 2026 Natural Science Foundation of Hunan Province, China (Grant No. 2026JJ80219), titled "Flexural Mechanism and Design Method of GFRP Bar-Reinforced Double-T UHPC-NC Composite Beams"; and (2) the 2025 Hengyang Science and Technology Innovation Program (Grant No. 202550037950), titled "Flexural Performance of Novel NC-UHPC-GFRP Composite Bridge Structures." The article processing charges (APC) were covered by Yuzhe Tang.

**Data Availability Statement:** The data presented in this study are available upon reasonable request from the corresponding author.

**Acknowledgments:** The authors acknowledge the support of Hunan Technical College of Railway High-Speed for providing the experimental site and facilities, and Central South University for technical assistance during the experimental program. During the preparation of this manuscript, the authors used Grammarly (Business Version) for English grammar checking and language polishing. The entire content was reviewed and revised by the authors, who take full responsibility for the published work.

**Conflicts of Interest:** The authors declare no conflicts of interest. The funders had no role in the design of the study; in the collection, analyses, or interpretation of data; in the writing of the manuscript; or in the decision to publish the results.

## References

**[1]** Richard P, Cheyrezy M. Ultra-high-performance concrete: a new material for the 21st century. Concr Int 1998;20(2):58-61.

**[2]** Graybeal BS. UHPC: a state-of-the-art report for the bridge community. Technical report FHWA-HRT-13-060. McLean, VA: Federal Highway Administration; 2013.

**[3]** Toutlemonde F, Resplendino J, editors. Designing and building with UHPFRC: state of the art and development. Proceedings of the international workshop, Marseille, 17-18 November 2009. Boca Raton: CRC Press; 2011.

**[4]** Jiao W, Lu G, Shao X, Liu J, Huang D. Design of bridge with 50 m-long simply-supported spans of U-shaped UHPC-NC composite girders. World Bridges 2024;52(5):1-8. doi:10.20052/j.issn.1671-7767.2024.05.001.

**[5]** Deng J, Li D, Zhou Y, Tian Z, Liu X. Creep shear stress on the interface of prestressed UHPC-NC composite beam. Appl Mech Eng 2024;41(5):1075-82. doi:10.11776/j.issn.1000-4939.2024.05.011.

**[6]** Resplendino J, Toutlemonde F, editors. Ultra-high performance fibre reinforced concrete: interim recommendations. Paris: Association Francaise de Genie Civil; 2002.

**[7]** International Federation for the Structural Concrete. fib Model Code for Concrete Structures 2020. Lausanne: fib; 2021.

**[8]** Ministry of Transport of the People's Republic of China. JTG 3362-2018: code for design of reinforced concrete and prestressed concrete highway bridges. Beijing: China Communications Press; 2018.

**[9]** Tong T, Yuan S, Wang J, Liu Z. The role of bond strength in structural behaviors of UHPC-NC composite beams: experimental investigation and finite element modeling. Compos Struct 2021;255:112914. doi:10.1016/j.compstruct.2020.112914.

**[10]** Wu Y, Zhang Y, Liu Y, et al. Experimental and numerical analysis on interfacial shear resistance of prefabricated UHPC-post-cast NC interface. Rail Constr 2023;63(9):48-53.

**[11]** Aaleti S, Sritharan S. Quantifying bonding characteristics between UHPC and normal-strength concrete for bridge deck application. J Bridge Eng 2019;24(6):04019041. doi:10.1061/(ASCE)BE.1943-5592.0001404.

**[12]** Carbonell Munoz M A, Harris D K, Ahlborn T M, Froster D C. Bond performance between ultrahigh-performance concrete and normal-strength concrete. J Mater Civ Eng 2014;26(8):04014031. doi:10.1061/(ASCE)MT.1943-5533.0000890.

**[13]** Luo J, Hu M, Ren X, Zhang B, Cao Q, Shu J, Yang S. Flexural behavior and crack width predictions of RC beams with different pre-damage degrees strengthened by UHPC. Eng Struct 2025;340:120742. doi:10.1016/j.engstruct.2025.120742.

**[14]** Haber Z B, Munoz J F, De la Varga I, et al. Bond characterization of UHPC overlays for concrete bridge decks: laboratory and field testing. Constr Build Mater 2018;190:1056-68. doi:10.1016/j.conbuildmat.2018.09.167.

**[15]** Zhou M, Hrynyk T D. Interface shear behaviour of ultra-high performance concrete under combined shear and lateral loads. Eng Struct 2026;346:121613. doi:10.1016/j.engstruct.2025.121613.

**[16]** Ye M, Li L, Jin W, Tang J, Yoo D Y, Zhou C. Interpretable ensemble machine learning models for predicting the shear capacity of UHPC joints. Eng Struct 2024;315:118443. doi:10.1016/j.engstruct.2024.118443.

**[17]** Ye M, Li L, Yoo D Y, Li H, Zhou C, Shao X. Prediction of shear strength in UHPC beams using machine learning-based models and SHAP interpretation. Constr Build Mater 2023;408:133752. doi:10.1016/j.conbuildmat.2023.133752.

**[18]** Tang Y, Wu Q. Bond-shear behaviour of the interface between precast UHPC formwork and cast-in-place NC. Build Mater Technol Appl 2025;(4):47-51.

**[19]** Tang Y, Fu M, Liu H. Impact factor analysis of UHPC-NC composite beam flexural load-bearing capacity. Highway Eng 2025;50(1):41-9,120. doi:10.19782/j.cnki.1674-0610.2025.01.006.

**[20]** Tang Y, Wu Q, Liu H. Study on flexural performance of corroded RC beams enhanced with ultra-high performance concrete. Build Mater Technol Appl 2026;(1):60-4. doi:10.3969/j.issn.1009-9441.2026.01.013.

**[21]** Men P, Chen F, Qin F, Peng X, Di J, Jiao H. Behavior of composite beams with UHPC-concrete composite slabs under negative bending moment. J Constr Steel Res 2025;227:109415. doi:10.1016/j.jcsr.2025.109415.

**[22]** Graybeal B, Bruhwiler E, Kim B S, Toutlemonde F, Voo Y L, Zaghi A. International perspective on UHPC in bridge engineering. J Bridge Eng 2020;25(11):04020094. doi:10.1061/(ASCE)BE.1943-5592.0001630.

**[23]** Tang Y. Strengthening of a heavy-haul railway simply-supported T-girder by external prestressing. Build Mater Technol Appl 2024;(1):32-7.

**[24]** Zhang Y, Wu Y, Qin Y, Zhu Y, Qiu J, Wang W. Experimental and analytical study on interfacial shear resistance of prefabricated UHPC-post-cast NC interface. Adv Struct Eng 2024;27(10):1622-34. doi:10.1177/13694332231196510.

**[25]** Toutlemonde F, Fouré B, Sorelli L, Baby F, Marchand P, Ulm F J. An overview of research advances from 2002 concerning UHPFRC, in view of updating the AFGC recommendations. In: Toutlemonde F, Resplendino J, editors. Designing and building with UHPFRC. Boca Raton: CRC Press; 2011. p. 639-64.

**[26]** Tayeh B A. Mechanical and permeability properties of the interface between normal concrete substrate and ultra high performance fiber concrete overlay. Constr Build Mater 2012;36:538-44. doi:10.1016/j.conbuildmat.2012.06.013.

**[27]** Smits J, François S, Van Gysel A, Molkens T. The effect of interlayer slip on the bending behaviour of composite beams: common background of the Eurocodes and missing links for concrete-concrete interfaces. J Build Eng 2026; in press.

**[28]** Du C, Liu X, Liu Y, Tong T. Prediction of the interface shear strength between ultra-high-performance concrete and normal concrete using artificial neural networks. Materials 2021;14:5707. doi:10.3390/ma14195707.

**[29]** Xu Z, Qin F, Yang Q, Peng X, Xu B. A review of research on the interfacial shear performance of ultra-high-performance concrete and normal concrete composite structures. Coatings 2025;15:414. doi:10.3390/coatings15040414.

**[30]** Jiang H, Wu K, Shen R, Li B, Xiao J, Mo F, Tian Y. Interfacial shear behavior between precast UHPC girder and cast-in-place NC slab with large groove and rebars. Struct Eng 2026;85:111041. doi:10.1016/j.istruc.2025.111041.

**[31]** Chen K, Lin Y, Gao J, Qi T, Wang W. Interfacial bond properties between cast-in-place UHPC and NC for composite girder bridges: experiments, analysis, and calculation methods. Struct Eng 2026;87:111407. doi:10.1016/j.istruc.2026.111407.